Received: 16 October 2023 | Revised: 22 March 2024 | Accepted: 7 May 2024

DOI: 10.1002/hipo.23610

RESEARCH ARTICLE

WILEY

A comparison of hippocampal and retrosplenial cortical spatial and contextual firing patterns

Dev Laxman Subramanian | Adam M. P. Miller | David M. Smith

Department of Psychology, Cornell University, Ithaca, New York, USA

Correspondence
David M. Smith, Department of Psychology, 236 Uris Hall, Cornell University, Ithaca, NY 14853, USA.
Email: dms248@cornell.edu

Funding information
National Institutes of Health, Grant/Award Number: MH083809

Abstract

The hippocampus (HPC) and retrosplenial cortex (RSC) are key components of the brain's memory and navigation systems. Lesions of either region produce profound deficits in spatial cognition and HPC neurons exhibit well-known spatial firing patterns (place fields). Recent studies have also identified an array of navigation-related firing patterns in the RSC. However, there has been little work comparing the response properties and information coding mechanisms of these two brain regions. In the present study, we examined the firing patterns of HPC and RSC neurons in two tasks which are commonly used to study spatial cognition in rodents, open field foraging with an environmental context manipulation and continuous T-maze alternation. We found striking similarities in the kinds of spatial and contextual information encoded by these two brain regions. Neurons in both regions carried information about the rat's current spatial location, trajectories and goal locations, and both regions reliably differentiated the contexts. However, we also found several key differences. For example, information about head direction was a prominent component of RSC representations but was only weakly encoded in the HPC. The two regions also used different coding schemes, even when they encoded the same kind of information. As expected, the HPC employed a sparse coding scheme characterized by compact, high contrast place fields, and information about spatial location was the dominant component of HPC representations. RSC firing patterns were more consistent with a distributed coding scheme. Instead of compact place fields, RSC neurons exhibited broad, but reliable, spatial and directional tuning, and they typically carried information about multiple navigational variables. The observed similarities highlight the closely related functions of the HPC and RSC, whereas the differences in information types and coding schemes suggest that these two regions likely make somewhat different contributions to spatial cognition.

KEYWORDS
context, hippocampus, memory, retrosplenial cortex, spatial

1 | INTRODUCTION

There is growing interest in the retrosplenial cortex (RSC) due to its role in memory and spatial cognition. The RSC is intimately interconnected with the hippocampus (HPC) via a complex array of direct and indirect projections involving the anterior thalamus, subiculum, and entorhinal cortex (Sugar et al., 2011; Van Groen, 1993; Van Groen & Wyss, 2003; Wyss & Van Groen, 1992), suggesting that these regions are all components of the brain's memory and navigations systems (Alexander, Robinson, et al., 2020;

Alexander, Robinson, et al., 2023; Miller et al., 2014; D. M. Smith et al., 2022). Consistent with this idea, damage to any of these regions produces profound memory and navigation impairments (Alexander, Robinson, et al., 2020; Bannerman et al., 2001; Mair, 1994; Scoville & Milner, 1957; D.M. Smith et al., 2022; Valenstein et al., 1987) and neurons throughout the circuit have been found to exhibit navigation-related firing patterns in rodents (Alexander & Nitz, 2015, 2017; Clark & Harvey, 2016; Hafting et al., 2005; Jankowski et al., 2015; Miller et al., 2019; O'Keefe & Dostrovsky, 1971; Taube, 1995). Recent studies have reported RSC neuronal firing patterns that bear a striking similarity to HPC firing patterns, including spatially localized firing which carries information about the location of the subject, the subject's current trajectory and the environmental context (Alexander & Nitz, 2015, 2017; Miller et al., 2019, 2021). These similarities are consistent with the idea that HPC representations become consolidated into the RSC (Alexander et al., 2018; Cowansage et al., 2014; De Sousa et al., 2019; Katche et al., 2013; Mao et al., 2018; Milczarek et al., 2018).

Despite these similarities, there is also considerable evidence for key functional differences between the two structures. For example, the RSC is involved in some instrumental learning tasks which do not require the HPC (Fournier et al., 2020, 2021; Gabriel, 1993; Robinson et al., 2011, 2014) and there are some kinds of neural responses that have been reported in the RSC, which are not thought to be prominent in the HPC, such as head direction (Cho & Sharp, 2001; Jacob et al., 2017) and egocentric boundary coding (Alexander, Carstensen, et al., 2020). These responses are prominent in other parts of this circuit, including the anterior thalamus and entorhinal cortex (Solstad et al., 2008; Taube, 1995), suggesting that the RSC may integrate information from several components of the memory and navigation circuit in a manner that the HPC does not.

Together, these findings suggest that the HPC and RSC may make related, but somewhat different contributions to spatial cognition. Moreover, the existing data from the RSC is suggestive of a distributed coding scheme that differs from the sparse coding seen in the HPC (e.g., Miller et al., 2021). Therefore, any comprehensive account of the circuit basis of memory and navigation will require a thorough examination of the similarities and differences in information processing in each structure. To that end, we combined archival data (Law et al., 2016; Miller et al., 2019, 2021) with new data to explicitly compare HPC and RSC spatial firing patterns during two commonly used behavioral tasks, open field foraging and continuous T-maze alternation.

2 | METHODS

2.1 | Subjects and surgical procedures

Subjects were 20 adult male Long-Evans rats and 1 adult female Long-Evans rat obtained from Charles River Laboratories, Wilmington, MA. Seven of the males were used in a study of firing patterns during open field exploration with a context manipulation (four used for RSC recordings and three used for HPC recordings). The remaining 13 males and the female were used in a study of firing patterns on a continuous T-maze (10 males used for RSC recordings, 3 males and one female used for HPC recordings). Some of these data were published previously (Law et al., 2016; Miller et al., 2019, 2021).

All rats underwent stereotaxic surgery to implant electrode microdrives, containing either 12, 16, or 24 tetrodes. All drives were custom fabricated to position tetrodes bilaterally in the region of interest (HPC: 4 mm posterior and 2.5 mm lateral from bregma, targeting the CA1 region; RSC: spanned approximately 4 mm along the rostrocaudal axis of the brain from 2 to 6 mm posterior to bregma and 1.5 mm lateral with the tetrodes angled 30° toward the midline, targeting the granular b region although a small number of recordings were also taken in the dysgranular subregion), except for one 12-tetrode drive (Harlan 12 Drive, Neuralynx Inc., Bozeman, MT), which targeted the right HPC. Coordinates were derived from the atlas of Paxinos and Watson (1998). Tetrodes consisted of four strands of either 17 μm platinum/iridium wires or 12.7 μm nichrome wires (California Fine Wire, Grover Beach, CA) platinum- or gold-plated to an impedance of 100–300 kΩ at 1 kHz. The rats were given an antibiotic (5 mg/kg Baytril) and an analgesic (5 mg/kg ketoprofen) prior to surgery. All procedures complied with guidelines established by the Cornell University Animal Care and Use Committee.

Rats were given 7 days to recover from surgery prior to lowering the tetrodes into the region of interest (35–70 μm daily) over the course of several days. For RSC recordings, tetrodes were lowered until a depth of at least 1 mm was reached to target the granular b subregion. For HPC recordings, the tetrodes were lowered until a majority of them reached the CA1 layer, as indicated by the presence of sharp wave ripples. Tetrodes were lowered after every recording session (~15–30 μm) in order to maximize the number of unique neurons recorded.

2.2 | Behavioral procedure and neuronal recording

2.2.1 | Open field foraging with context manipulation

After recovery from surgery, the rats were acclimated to the apparatus and trained to forage for chocolate sprinkles. During the daily recording sessions, rats foraged for chocolate sprinkles in two distinct environmentally defined contexts (PVC boxes measuring 100 cm × 100 cm × 50 cm deep) that differed in the color of the box (black or white), the color of the surrounding environment (white curtains or black walls of the room), background masking noise (pink or white noise), and ambient odor left by wiping the boxes with baby wipes of different scents (Rite Aid, Inc.). White curtains were used with the black box to create a color contrast to help differentiate the two contexts. This manipulation also obscured the rat's view of distal objects in the experimental room (e.g., the recording computer). The rats were given four 12 min trials, two in each context. Between trials, the rat was placed in an opaque cylinder (30 × 65 cm) for ~3 min while the experimenter changed the contexts.

2.2.2 | Continuous T-maze

For the continuous T-maze experiment, the rats were trained on a black PVC T-maze (120 cm long stem × 100 cm wide × 68 cm above the floor) with metal reward cups embedded in the ends of the arms through which chocolate milk (0.2 ml, Nestle's Nesquik) was delivered via an elevated reservoir controlled by solenoid valves activated by foot-pedal switches. The maze was located in the center of a circular arena enclosed by black curtains with distinctive visual cues. A continuous background masking noise (white noise) was played from a speaker located directly above the maze. After acclimation to the maze, rats were trained on a continuous spatial alternation task in which the rats were rewarded only if they approached the reward location (left or right) which was opposite from the previous trial. Both cups were baited on the first trial. Entries into the same arm as the previous trial were scored as an error and were not rewarded. Rats were not allowed to correct their errors and were gently ushered back if they left the continuous alternation route. Rats were given 40 trials/day until they achieved a criterion of 90% correct on two consecutive sessions. After achieving this criterion, neuronal activity was recorded during asymptotic performance sessions.

2.3 | Data collection

Neuronal spike data and video recordings of the rat's location and head direction were collected using the Cheetah Digital Data Acquisition System (Neuralynx, Inc.). Neuronal recordings were filtered at 600 Hz and 6 kHz, digitized and stored to disc along with timestamps for offline sorting (SpikeSort3D, Neuralynx, Inc.). The rat's position and head direction were monitored by digitized video (sampled at 30 Hz) of two LEDs attached to the head stage. Head direction was calculated by taking the angle between the two LEDs, and was independent of the rat's direction of movement. For the open field dataset, a total of 143 RSC neurons were recorded from 4 rats (97 putative pyramidal neurons and 46 interneurons, classified as in Brennan et al., 2020). A total of 328 neurons were recorded in the CA1 region of HPC from 3 rats (320 pyramidal neurons and 8 interneurons). For the T-maze experiment, a total of 309 RSC neurons (201 pyramidal neurons and 108 interneurons) were recorded from 10 rats. A total of 607 neurons were recorded from CA1 of 4 rats (521 pyramidal neurons and 86 interneurons). We limited our analysis to pyramidal neurons in the HPC because interneurons have well-known differences in firing characteristics and spatial coding (Fox & Ranck, 1981; Frank et al., 2001; Kubie et al., 1990). However, although RSC pyramidal and interneurons can be sorted according to spike width (Brennan et al., 2020), the two cell types do not fall into distinct fast- and slow-spiking cell types during behavior, and we found that the firing characteristics of the two putative cell types were similar, unlike in the HPC (see Supplementary Figure 1). We also performed each of our major analyses with RSC pyramidal and interneurons separated and found no cases where the inclusion of RSC interneurons made a substantive difference in the outcome, so we included all RSC neurons in the final analyses we report here. This approach is consistent with previous studies of RSC firing patterns (Alexander, Carstensen, et al., 2020; Alexander & Nitz, 2017; Miller et al., 2019, 2021).

2.4 | Histology

After completion of the study, rats were transcardially perfused with 4% paraformaldehyde in phosphate buffered saline. Brains were removed and stored for at least 24 h in 4% paraformaldehyde before being transferred to a 30% sucrose solution for storage until slicing. Coronal sections (40 μm) were stained with 0.5% cresyl violet for visualization of tetrode tracks. Tetrode positions were identified using depth records noted during tetrode lowering and tracks observed in the stained tissue.

2.5 | Data analysis

2.5.1 | Firing rate maps and measures of neuronal firing characteristics

The floors of the open field and T-maze were divided into 2.5 × 2.5 cm square pixels, and the firing rate of each neuron was determined by dividing the total number of spikes in each pixel by the time spent in the pixel. Spatial firing rate maps were smoothed by convolution with a 7 × 7 pixel Gaussian kernel with unity sum. We also computed several measures of individual neuronal firing characteristics, including the average firing rate, sparsity index, information content, mutual information, and the correlation between running speed and firing rate.

2.5.2 | Sparsity index

Sparsity index indicates the relative proportion of the experimental area (open field or T-maze) in which the cell fired. This is a measure of lifetime sparseness, computed as:

$$\textbf{Sparsity index} = \sum \left(P_i{}^{*} R_i{}^{2}\right)/R^{2}.$$

where P_i is the probability of occupancy of bin i, R_i is the mean firing rate in bin i, and R is the overall mean firing rate (Markus et al., 1994).

2.5.3 | Information content

Information content was used to measure how much information the firing of a neuron provides about the location of the rat in bits/spike (Skaggs et al., 1993).

$$\textbf{Information content} = \sum P_i{}^{*} (R_i/R)^{*} log_2(R_i/R).$$

where i is the bin number, P_i is the probability for occupancy of bin i, R_i is the mean firing rate for bin i, and R is the overall mean firing rate.

2.5.4 | Mutual information

Mutual information was used to measure how much information about the firing activity of the neuron is provided by knowing the location of the rat. A location-specific information measure called "Positional information (I_{pos})" is first obtained from the spike counts at each location within each time window (Olypher et al., 2003). I_{pos} gives a measure of the extent to which uncertainty about the spike count is reduced given the rat's location. It takes into account any differences in firing for separate visits to each location, and therefore reflects the reliability of a particular firing rate at any given location.

$$\textbf{Positional information}, I_{pos}(x_i) = \Sigma P(k|x_i)^* \log_2[P(k|x_i)/P_k].$$

where P_k is the probability of observing k spikes and $P(k|x_i)$ is the conditional probability of observing k spikes at location x_i. The mean of all $I_{pos}(x_i)$ values is computed to produce the overall measure of mutual information between the locations and spike counts, measured in bits:

$$\textbf{Mutual information} = \Sigma P_{xi}{}^* I_{pos}(x_i).$$

where P_{xi} in the probability the rat is in location x_i.

2.5.5 | Spatial coding at the population level

In order to assess spatial coding at the population level, we combined the neurons from all rats and recording sessions into a single population and used a minimum distance classifier to predict the location of the rat based solely on neuronal firing patterns. Populations constructed from neurons in different rats cannot reflect dynamic interactions among the neurons within the population, but they are nevertheless useful for examining how much information can be encoded by a collection of neurons that exhibit the various types of responses that are characteristic of a given brain region.

Population firing rate vectors for every 250 ms time bin during the recording session were constructed using z-scored firing rates to control for differences in baseline firing, which can make population measures overly sensitive to a few neurons with high firing rates. Time bins from each session were then sorted according to which spatial bin (36 bins) the rat was in during that time. Larger spatial bins (17 cm × 17 cm) were used for this analysis so that a sufficient number of visits could be accumulated to train the classifier. Because rats differed in the number of visits they made to each pixel, only 20 visits (250 ms time bins) from each spatial bin were included in the analysis. When a rat made more than 20 visits to a spatial bin, we preferentially selected visits where the average spatial location of the rat was closer to the center of the bin to avoid including time bins that contained spiking activity from adjacent spatial bins. This resulted in 720 firing rate vectors (6 pixels × 6 pixels × 20 time bins), representing the instantaneous population firing patterns observed across all the spatial locations.

We then computed the mean firing rate vector for each spatial bin, reflecting the average population firing pattern at each location, and we classified each of the 720 individual vectors into spatial bins according to which average vector was the most similar (i.e., the smallest Euclidean distance). The average vectors were always computed without the test sample. This procedure yielded a measure of the degree to which instantaneous population firing patterns matched the typical (average) firing pattern for a given location. Classification accuracy was calculated as the percentage of instances when the firing pattern was most similar to the correct spatial bin. In order to compare classification accuracy across regions, we randomly subsampled the firing rates of 100 neurons from the total population in each region 1000 times and then computed the average accuracy across those samples. In order to examine classification accuracy at different population sizes, we randomly subsampled populations of each size. Similar procedures were used for all classifier analyses.

2.5.6 | Context-dependent spatial coding

In order to determine whether individual neurons carried information about the context in their spatial firing patterns, we computed pairwise pixel by pixel correlations (Pearson's r) of the firing rate maps for the four trials of the open field task. The resulting r values were averaged to create one correlation reflecting within-context similarity and one reflecting between-context similarity for each neuron. We also assessed the context dependency of spatial firing patterns at the population coding using a minimum distance classifier, as described above. However, for this analysis, we used the average firing rate map for one trial and attempted to classify sample population vectors from another trial, either in the same context or in the other context. Classification accuracy is high for trials that have similar spatial firing patterns, but low for trials that have different firing patterns. Each sample population vector was therefore compared to the average rate map for the other trial in the same context and to the rate map for a trial in the opposite context.

2.5.7 | Rate coding of the contexts

In order to determine whether the overall firing rate of the neurons carried information about the context, we attempted to predict the current context from the population firing patterns using a minimum distance classifier. For this analysis, we binned the firing rates into successive 250 ms time bins without regard to the rat's location in the environment, yielding 2880 population vectors for each 12 min trial. We then computed the Euclidean distance between each of these population vectors and the mean firing rate vector for the white context and the black context and assigned the sample vector to the

closest match (smallest distance). This analysis asks how well the firing rates match the average for each context at each timepoint in the trial, regardless of the rat's location or ongoing behavior. Decoding success reflects how reliably the firing rate at each of these timepoints differentiates the contexts.

2.5.8 | Directional coding

For each neuron, we binned the firing rate into 60 directional heading bins of 6° width, smoothed them with a sliding average of three bins, and generated a polar plot. The peak directional firing rate was defined as the maximal firing rate in the smoothed tuning curve. Only the neurons that had a peak directional firing rate exceeding 1 Hz were included in the analyses (HPC $n = 95$, RSC $n = 139$). We assessed the quality of the directional coding by computing the mutual information between the firing rate and the head direction for each neuron. Similar to the analysis of spatial firing, this measure reflects how reliable and unique the neuron's firing rate was for each directional heading. As an additional measure of the reliability of directional coding, we correlated the directionally binned firing rates for separate visits to the same context (Black 1 and Black 2, White 1 and White 2). We also used a minimum distance classifier to predict the rat's head direction from the population firing patterns. Similar to above-described analyses, we generated population vectors and sorted them into directional bins according to the Euclidean distance (60 population vectors of 250 ms time bins for each of 20 directional bins of 18° width).

2.5.9 | Linear–nonlinear model

We used the linear–nonlinear (L–N) model developed by Hardcastle et al. (2017) to assess the degree to which multiple behavioral variables might influence the firing rates of HPC and RSC neurons. This model is useful for assessing the firing properties of neurons that respond to complex combinations of behavioral and experimental variables because it allows for the independent assessment of how each variable or combination of variables influences neuronal firing. Briefly, the model estimates the firing rate of an individual neuron as a function of each variable of interest (spatial position, context, head direction, running speed, acceleration, and angular velocity). For each neuron, one model was generated for every possible combination of variables and then these models were compared against one another by computing the log-likelihood of held-out data under the model, and penalizing models that over-fit the data. Neurons were then classified in terms of which set of variables were significantly encoded.

2.5.10 | Trajectory and reward location coding on the T-maze

We determined whether HPC and RSC neurons exhibited differential firing for left and right turn trajectories on the T-maze by examining firing on the stem of the maze. For each neuron, we computed a *t*-score (Student's *t*), which reflects the trial-by-trial reliability of firing rate differences for left and right turn trials, and generated distributions of these values for each brain region. We also assessed trajectory coding at the population level. We first examined the degree to which populations in each region differentiated left and right trajectories by generating a population vector for each traversal of the stem and computing the Euclidean distance between that population vector and the average population vector for all left traversals and all right traversals. We then used a minimum distance classifier to predict whether sample population vectors (250 ms time bins) occurred during a left or right traversal. In order to ensure that variation in behavior could not have caused apparent differences on left and right traversals, these analyses were restricted to correct trials with stem runs that did not involve pauses or deviations from smooth locomotion (see Miller et al., 2019).

We determined whether HPC and RSC neurons differentially encoded the two reward locations (left and right) using a similar approach. For these analyses, we focused on the firing occurring during the 2 s following arrival at each reward location, while rats were stationary and consuming the reward. As described above, we computed a *t*-statistic for each neuron. We then generated population vectors for each trial, computed the Euclidean distance between each population vector and the average vector for the same- and opposite reward locations (left and right), and applied a minimum distance classifier to predict whether population vectors occurred at the left or right reward locations.

3 | RESULTS

3.1 | Spatially localized firing

We compared neuronal firing characteristics in the HPC and RSC from two commonly used behavioral tasks, open field foraging with an environmental context manipulation and a continuous T-maze alternation task. Direct comparison of the spatial firing characteristics of RSC and HPC neurons is challenging because widely used measures for describing HPC firing characteristics are optimized for neurons that have well-defined place fields and very low firing rates elsewhere in the environment. However, RSC neurons frequently exhibit large areas of elevated firing with indistinct boundaries and high background firing rates, which makes classification criterion arbitrary and overly sensitive to the classification parameters. Therefore, we did not attempt to define place field boundaries or classify neurons as to whether they had spatial firing or not. Instead, we adopted a strategy of comparing the distributions of various measures that characterize the neuronal firing patterns and we provide illustrative examples of various response types. We also employed a decoding approach in which we combine all the neurons from all the rats into a single population and attempt to predict the rat's location or other variables solely from the population firing patterns (see Methods, Section 2.5.5).

HPC neurons had uniformly low firing rates in both tasks, whereas RSC neurons varied widely but exhibited much higher

average firing rates (Figure 1e, 0.78 ± 0.03 Hz in HPC compared to 29.88 ± 1.09 Hz in RSC in the open field). This can readily be seen in the firing rate maps (Figure 1a,b) where HPC neurons exhibit well-defined regions of elevated firing (place fields) with background firing rates near zero whereas RSC neurons typically fired across wide areas of the apparatus. Consistent with this, HPC firing was much sparser

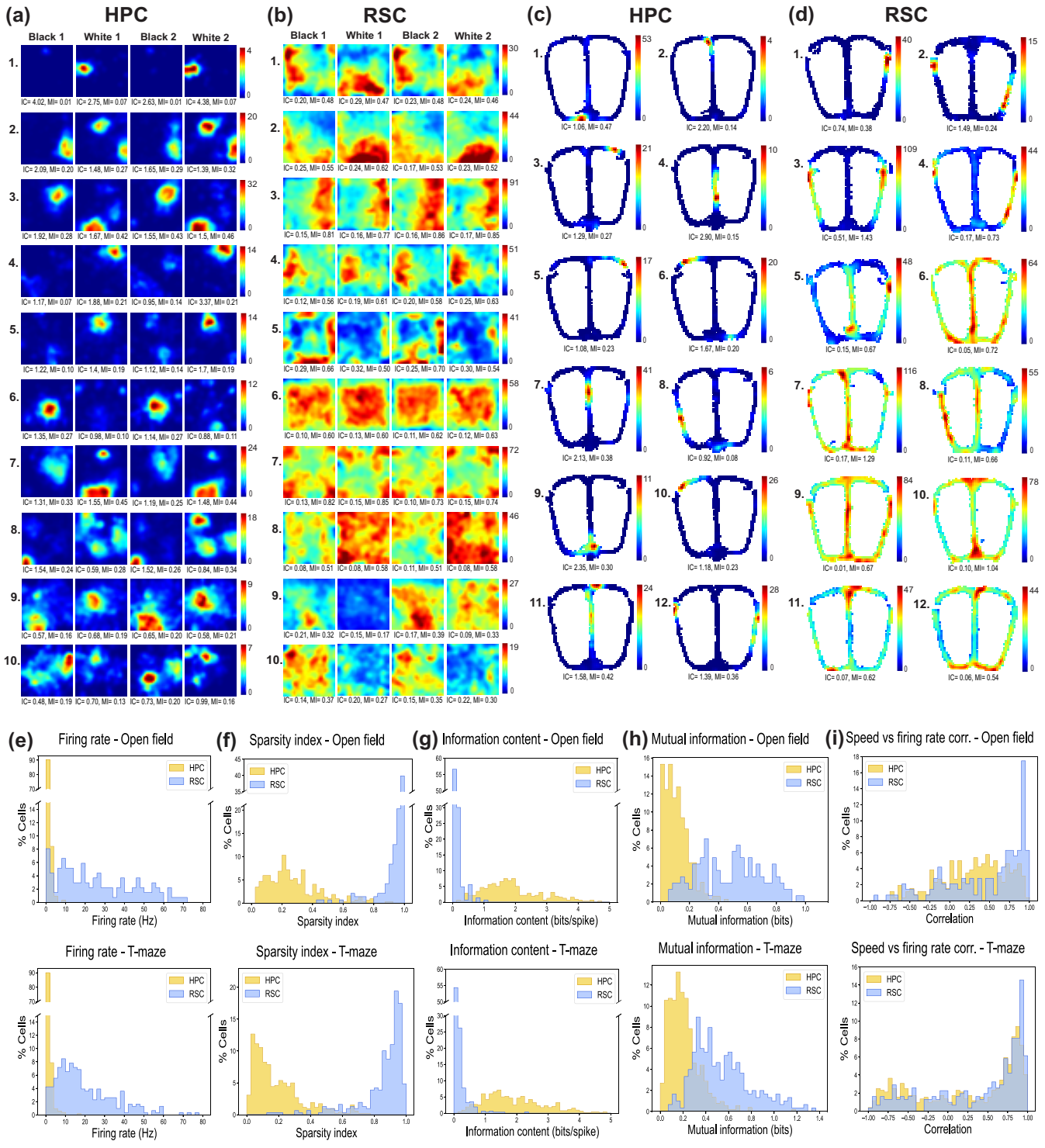

FIGURE 1 Spatial firing rate maps from the hippocampus (HPC) (a, c) and retrosplenial cortex (RSC) (b, d) are shown to illustrate the range of firing patterns observed during open field foraging task and the continuous T-maze. Most HPC neurons exhibited clear place fields which differed for the black and white contexts, whereas RSC neurons exhibited a range of spatial firing patterns, generally involving large areas of elevated firing (see text). Each firing rate map includes the information content (IC) and mutual information (MI) score for that neuron. Plots E-I illustrate the distributions of various measures of firing characteristics for HPC (yellow) and RSC neurons (blue). Data are shown separately for the open field foraging task and the T-maze task.

than RSC neurons (Figure 1f). The sparsity index reflects the proportion of the area in which the cell fired, so lower values indicate sparser firing patterns. RSC neurons exhibited a wide range of spatial firing patterns. In the open field, this included clearly identifiable regions of elevated firing which were larger than HPC place fields and had less distinct boundaries (Figure 1b, plots 1–4). We did not perform a detailed analysis of egocentric boundary coding, which has been reported previously (Alexander, Carstensen, et al., 2020), but we did observe several clear examples which were consistent with the previous report (Figure 1b, plot 5). We also observed neurons with reduced firing near the walls (plot 6) as well as elevated or reduced firing near the corners of the box (e.g., plot 7). On the T-maze, we occasionally observed relatively compact HPC-like place fields (Figure 1d, plots 1–2), but these were never observed in the open field, suggesting that the behavioral constraints of the maze task (e.g., speed, heading direction, turns) may influence spatial firing. We also observed symmetrical firing on the left and right halves of the maze (e.g., plot 3) and elevated firing at turns and junctions on the maze (e.g., plots 10–12, also see Alexander & Nitz, 2015; Cho & Sharp, 2001). More commonly, we observed widespread firing with large areas of reliably elevated firing (plots 6–12), as in the open field. The firing of neurons in both regions was often correlated with running speed on the T-maze, but a substantial percentage of RSC neurons also showed strong running speed correlations in the open field (Figure 1i).

Various approaches have been used to measure how much information about the location of the subject is carried by the firing patterns of individual neurons. Information content, measured in bits/spike, reflects how much information each spike conveys about the current location of the subject (Skaggs et al., 1993). This measure increases when place fields are smaller rather than larger, and when the difference between the in-field and out of field firing rates are large. Unsurprisingly, information content is much higher in HPC neurons (Figure 1g), which have compact place fields and low background firing. In contrast, mutual information takes into account the firing rate at all locations in the environment, including locations with no firing, and it accounts for the reliability of firing at each location (Olypher et al., 2003). This analysis yields high information values for a given location when the firing rate is both unique to that location and is reliably observed across multiple visits, even when there are not well-defined place fields (see Wilent & Nitz, 2007 for a discussion of this measure). Consequently, mutual information is much higher in the RSC than the HPC, where mutual information values are low because HPC neurons carry little information about locations outside of their place field (Figure 1h). Thus, these two measures, information content and mutual information, illustrate a key difference between spatial coding in the HPC and RSC, with the former employing punctate place fields and the latter employing reliably distinct firing rates distributed widely across the environment.

Another way of assessing the quality of spatial representations is to ask how well you can predict the location of the subject based solely on the population firing patterns. We performed this analysis on the open field data, where spatial firing patterns are less likely to be influenced by behavioral variables such as heading direction and running speed, which are confounded with location in maze tasks. To assess this, we computed the average population firing pattern for each pixel of the open field (see Methods, Section 2.5.5). We then repeatedly selected 250 ms samples, computed the Euclidean distance to each of the possible locations and assigned the sample to the location with the smallest distance (i.e., a minimum distance classifier, Figure 2a). We could predict the rat's current location based on the firing patterns from either region at rates far better than chance (HPC accuracy = 59.09% ± 0.07, one-sample t test of 1000 randomly selected populations of 100 neurons compared to chance = 2.78%, $t(999) = 797.54$, $p < .001$; RSC accuracy = 51.36% ± 0.07, $t(999) = 743.27$, $p < .001$). In order to examine the relationship between population size and classification accuracy, we repeated this procedure for randomly selected subsets of our neurons and found that classification accuracy was well above chance even for populations as small as 20 neurons and increased with increasing population size (Figure 2b). Classification accuracy was higher for HPC neurons across all population sizes (e.g., for 100 neurons $t(1998) = 80.33$, $p < .001$, Figure 2b inset).

3.2 | Context discrimination

The HPC and RSC are thought to encode information about the environmental context, but the mechanisms of representing and differentiating contexts may differ across the two regions. The HPC is thought to represent contexts by generating unique spatial firing patterns for each context (D. M. Smith & Bulkin, 2014), a result that can readily be seen in our data (Figure 1a). Many RSC neurons also exhibited reliably different spatial firing patterns in different contexts (e.g., Figure 1b, plots 1, 2, 5, 9). However, context dependency was quite variable across the RSC population, and many neurons did not exhibit obvious differences in spatial firing between contexts (e.g., Figure 1b, plots 3, 4, 6, 7). We examined the capacity for spatial coding of contexts by computing pixel-by-pixel spatial correlations comparing the two visits to the same context (within) and visits to different contexts (between) for each neuron (Figure 3a). A two-way mixed ANOVA found a main effect of context condition (within vs. between, $F(1,437) = 846.56$, $p < .001$) and a context condition by brain region interaction ($F(1,437) = 188.33$, $p < .001$). Post hoc tests indicated that within-context spatial correlations were higher than between-context correlations in both regions, suggesting that both HPC and RSC spatial firing patterns differentiate contexts. However, this effect was weaker in the RSC, where within-context correlations were attenuated ($t(437) = 0.16$, $p < .001$, Tukey–Kramer test) and between-context correlations were elevated ($t(437) = 0.21$, $p < .001$), relative to the HPC. This result suggests that HPC spatial firing is more consistent for repeated visits to the same context and more thoroughly orthogonalized for visits to different contexts, relative to the RSC. This can readily be seen when within- and between-context correlations are plotted for each neuron (Figure 3b). Note that the HPC neurons form a noticeable vertical band near zero on the x-axis, indicating uncorrelated firing patterns in different contexts for many

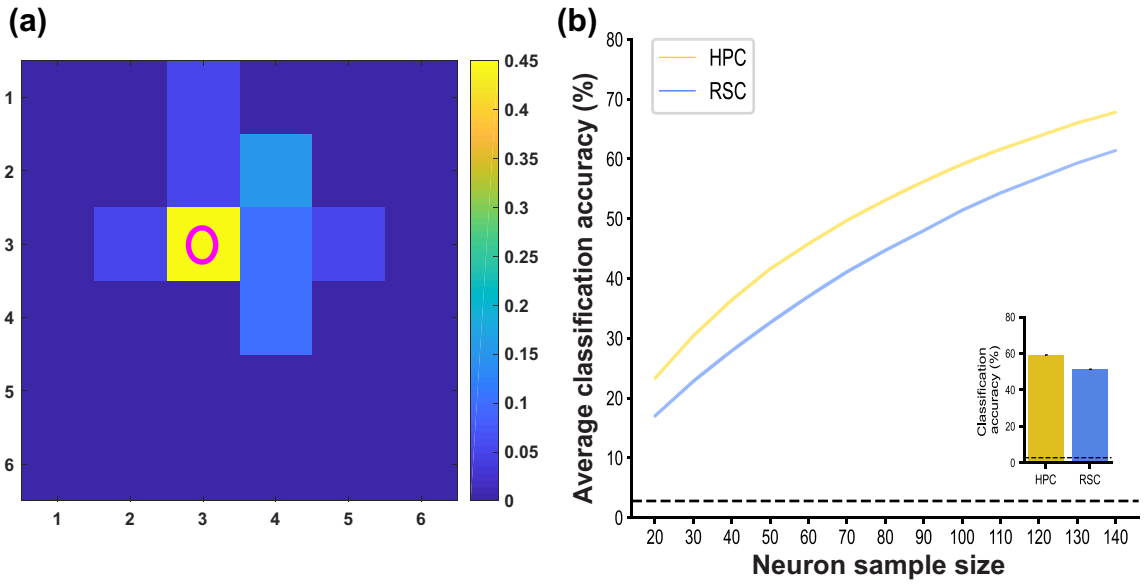

FIGURE 2 The location of the rat could readily be decoded from population firing patterns in both the hippocampus (HPC) and retrosplenial cortex (RSC). Plot (a) illustrates the probability map for an example RSC population (250 ms samples taken while the rat was in pixel 3:3). Colors indicate the proportion of classifications for each pixel based on the smallest Euclidean distance. For this example, most of the sampled population firing patterns best matched the rat's actual position (pink circle) and most of the incorrect classifications indicated nearby pixels. Plot (b) illustrates the classification accuracy across different population sizes of HPC and RSC neurons, sub-sampled from the total neuronal population in each region (mean ± SEM indicated by the thickness of the line). The dashed line represents chance accuracy (2.78%). The average classification accuracy values for a population size of 100 neurons are shown in the inset (error bars are plotted but are difficult to see, so SEM values are given in the text).

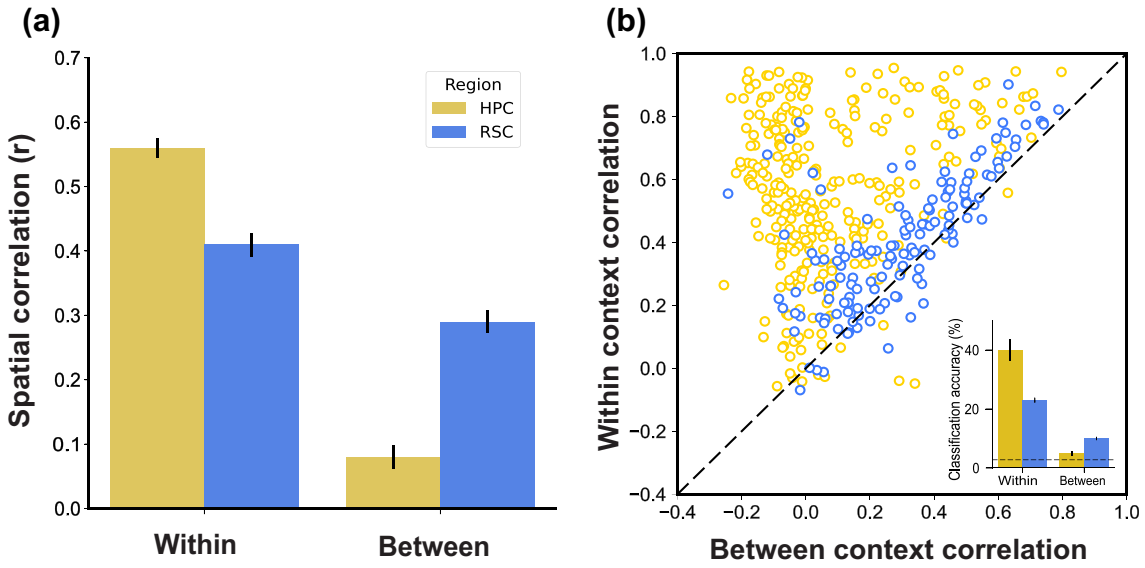

FIGURE 3 Context-specific spatial firing. Pixel-by-pixel spatial correlations (Pearson's *r*) comparing trials taking place in the same context (within) and trials taking place in different contexts (between) for the hippocampus (HPC) and retrosplenial cortex (RSC) are shown in plot (a). Neurons in both regions exhibit context-dependent spatial firing patterns, as indicated by greater within-context correlations as compared to between-context correlations, but this was reduced in the RSC (see text). In plot (b), the within- and between-context *r* values are plotted against each other for each neuron (circles). Note that most of the dots are above the unity line, indicating that the spatial firing patterns were more similar for trials in the same context than for trials that took place in different contexts. However, the pattern of dots is different for the two regions, with HPC neurons exhibiting a notable vertical band at zero on the x-axis, consistent with orthogonalization, and RSC neurons distributed along the unity line. Spatial location classification accuracy is shown in the inset. The classifier was trained on one trial and tested on data from a different trial, either in the same context or the opposite context. Population representations showed the same pattern of results as the spatial correlation data for individual neurons (plot a).

neurons. In contrast, the values for RSC neurons are distributed along a diagonal band just above the unity line, indicating that spatial firing patterns could have high similarity in different contexts. However, it is notable that spatial firing patterns were nearly always more similar for visits to the same context than for visits to different contexts (dots above the unity line).

A decoding strategy can also be used to examine context-specific spatial firing patterns. We trained a minimum distance classifier on the spatial firing patterns from one trial and then attempted to decode the rat's position in another trial, either in the same context or in a different context. If spatial firing patterns are consistent across trials decoding accuracy will be high, but if firing patterns differ then accuracy will be low. A two-way mixed ANOVA of average decoding accuracy produced the same pattern of results seen with the spatial correlations (Figure 3b, inset). There was a main effect of context condition (within vs. between, $F(1,1998) = 253{,}883.26$, $p < .001$), indicating that decoding across trials from the same context was more accurate than decoding across different contexts, and a significant interaction of the brain region and context conditions ($F(1,1998) = 52{,}211.53$, $p < .001$). Post hoc tests found that same-context decoding accuracy was greater in the HPC than in the RSC ($t(1998) = 0.17$, $p < .001$, Tukey–Kramer test) and between-context decoding accuracy higher in the RSC than the HPC ($t(1998) = 0.05$, $p < .001$).

Contexts can be encoded by distinct spatial firing patterns, as described above, but they can also be differentiated using a rate code. Previously, we reported that many RSC neurons fired at systematically different rates in the black and white contexts, regardless of the rat's spatial position in the environment (Miller et al., 2021, also see Carstensen et al., 2021). In the HPC, the term "rate remapping" has been used to describe changes in a neuron's firing rate without changes in the location of the place field, which is thought to occur in response to relatively small changes in the environment (Leutgeb et al., 2005). We saw little evidence of this form of rate remapping in HPC neurons here, possibly because our manipulation involved large-scale changes in the context rather than the limited environmental changes of the Leutgeb et al., 2005 study. However, HPC neurons often had a place field in one context with little firing in the other. This naturally results in many neurons having systematically different firing rates in the two contexts, which could also serve as a rate code.

We compared rate coding in the two regions by computing the firing rate of each neuron in 10-s time bins for each of the four trials, without regard to the rat's location in the environment. Examples of rate coding by individual neurons are shown in Figure 4a,b. In the RSC, neurons could have large firing rate differences with or without spatial specificity. In contrast, none of the HPC neurons had a clear rate code without also exhibiting spatial specificity. Plots of all neurons sorted by firing rate in the black context are shown in Figure 4c. We attempted to identify the current context from the population firing patterns using a minimum distance classifier and found that classification accuracy was significantly above chance (50%) in both regions. However, classification was significantly better in the RSC than the HPC (Figure 4d, HPC accuracy = 79.19% ± 0.15, RSC accuracy = 87.03% ± 0.16, $t(1998) = 50.67$, $p < .001$) and this was true across all population sizes (not shown). For example, the classification accuracy obtained from a random sampling of 50 RSC neurons was as good as the accuracy obtained from ~90 HPC neurons. This was likely because although many HPC neurons fire at different rates, they do so primarily within their circumscribed place field and firing rates outside the place field are near zero in both contexts. This can be seen in the patchiness of the color plots of firing rate over time (Figure 4c) and the variability of the single neuron plots (Figure 4a). Consistent with this, the variance of the time binned firing rates was twice as large in the HPC as in the RSC (mean HPC: 0.99 ± 0.002, mean RSC: 0.49 ± 0.02, $t(144.8) = 24.63$, $p < .001$, Welch's t test for unequal variances).

3.3 | Directional firing

Directionally selective firing has been reported extensively in the RSC (e.g., Zhang et al., 2022) and sometimes in the HPC (Jercog et al., 2019; Leutgeb et al., 2000). We examined directional firing in the open field where behavior is less constrained than in the T-maze. Consistent with previous reports, we found widespread directional firing in the RSC but only weak directional firing in the HPC. Similar to spatial firing patterns, RSC directional firing often took the form of high baseline firing rates with reliably higher firing across a range of preferred head directions (Figure 5a). Notably, RSC directional coding was present in neurons that fired throughout the environment (e.g., Figure 5a, plots 1–3), but could also occur in conjunction with spatially localized firing (e.g., Figure 5a, plot 4).

Consistent with previous reports (Zhang et al., 2022), although all directions were represented in the population (Supplementary Figure 2, plot d), RSC neurons often exhibited two (Figure 5c, plots 1, 3) or four preferred directions (Figure 5a, plots 3, 5, 6). Figure 5f illustrates the firing rates of all HPC and RSC neurons, with the peak firing aligned to zero and sorted by the amount of multi-directionality exhibited by each neuron (computed as in Zhang et al., 2022). Note the additional firing at 90°, 180°, and 270° from the primary peak. In many cases, directional firing was related to particular spatial locations. For example, in Figure 5a, plot 5, the neuron had preferred directions aligned to the corners of the box, along with elevated firing in the corners. The neuron in Figure 5a, plot 6 is an egocentric boundary cell (Alexander, Carstensen, et al., 2020), which fired when the rat was near the wall with the wall to the rat's left.

As with spatial coding, we took a multipronged approach to assessing the quality of directional coding. First for each neuron, we binned the firing rates into 6° directional bins and computed the mutual information score reflecting how reliably the firing rates differ across directions. We found that, on average, RSC neurons carried significantly more information about head direction than HPC neurons (Figure 5d, HPC mean = 0.085 ± 0.003, RSC mean = 0.25 ± 0.01, $t(163.35) = 15.21$, $p < .001$, Welch's t test for unequal variances). We also examined the reliability of directional tuning by correlating the tuning curves for the first and second visit to each context and found that directional firing patterns were significantly more correlated in

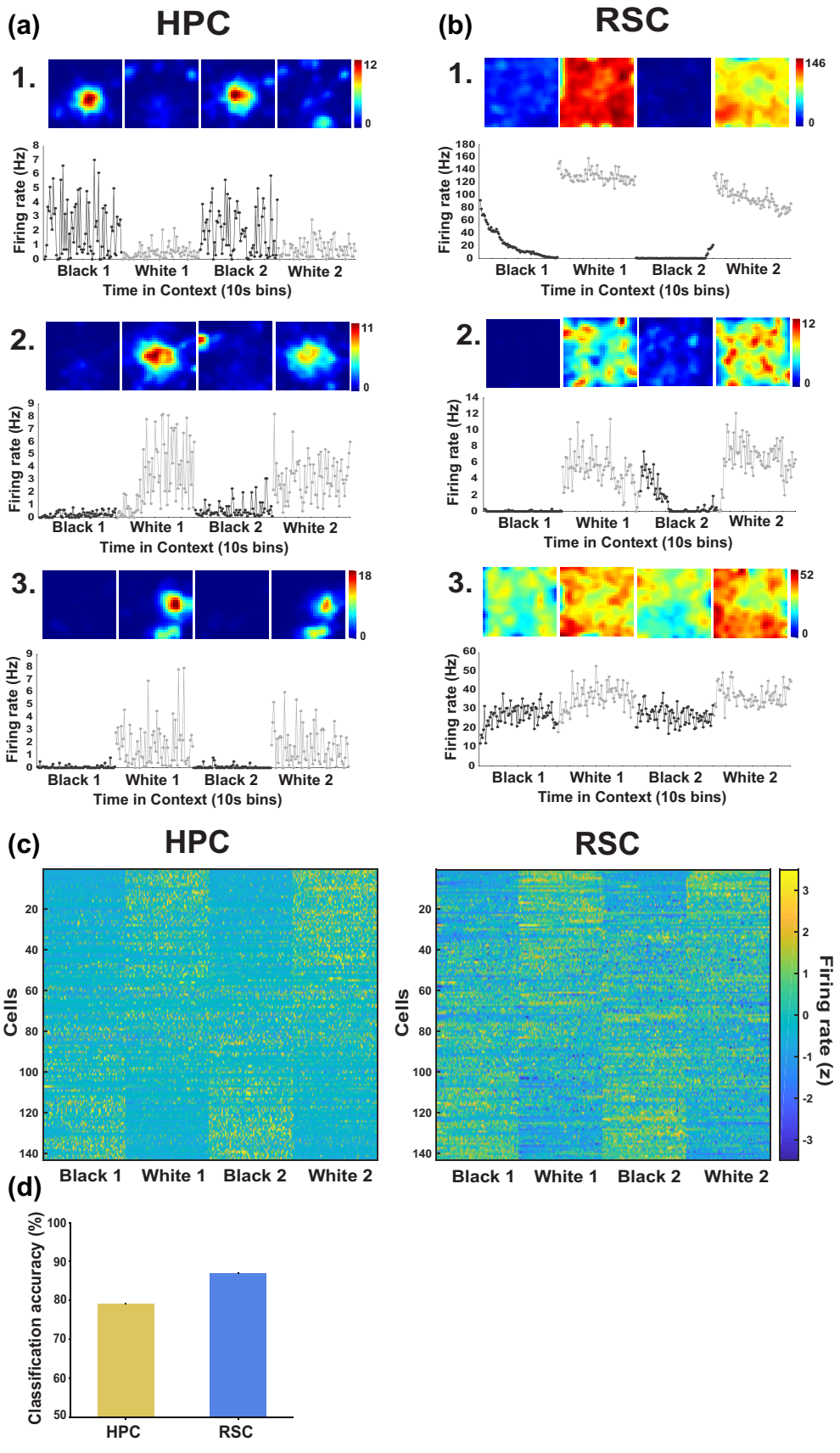

FIGURE 4 Rate coding of the contexts. Plots (a) and (b) show example neurons illustrating how firing rate differences may differentiate contexts. For each neuron, spatial firing rate maps are shown above and average firing rate in successive 10-s bins throughout the duration of each 12-min trial is shown in the line plots below. In the hippocampus (HPC), the neurons fire at noticeably different rates in the black and white contexts due to the presence of a place field in one context, but not the other. This creates variability in the time-binned data because the neurons are generally silent when the rat is not in the place field. In the retrosplenial cortex (RSC), neurons could exhibit reliably different firing rates without spatial specificity. In extreme cases (e.g., plots b1-2), this results in continuously different firing rates for each context which do not depend on spatial location within the environment. This pattern can also be seen in plot (c), which illustrates the time-binned firing rates (10 s bins) across the four trials for HPC and RSC neurons, one row per neuron, sorted by firing rate in the black context. Note the presence of black-preferring and white-preferring neurons in both regions, although the HPC firing is more patchy than RSC firing. Plot (d) illustrates the average classification accuracy for decoding the current context (black or white) from population firing patterns in each region. Error bars are plotted but are difficult to see, so SEM values are given in the text.

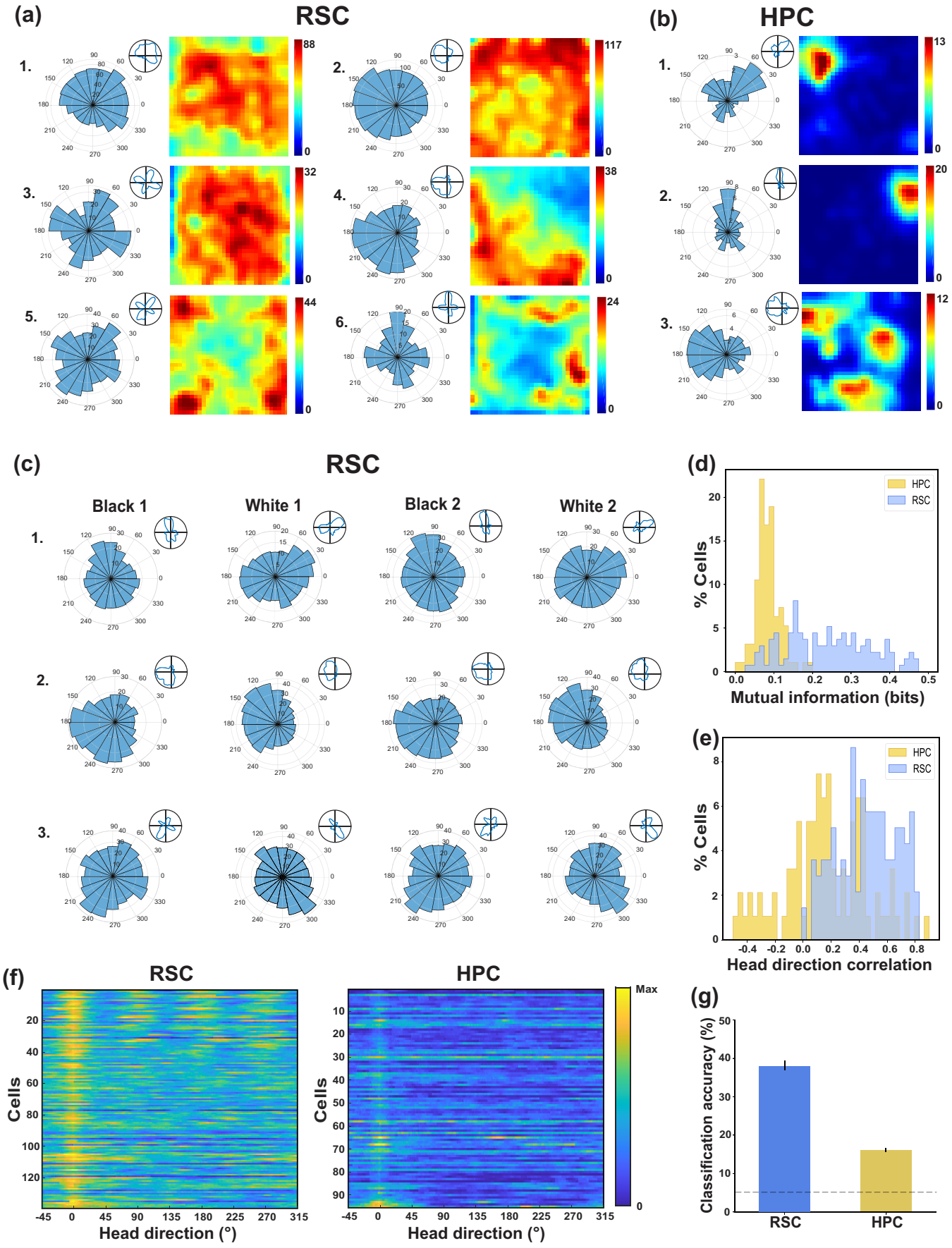

FIGURE 5 Legend on next page.

the RSC as compared to the HPC (Figure 5e, $r = .45$ in RSC, compared to 0.16 in HPC, $t(153.17) = 8.1$, $p < .001$). We did not use the commonly employed Rayleigh statistic because it is optimized for neurons with high firing rates at the preferred direction with very low baseline firing rates (e.g., anterior dorsal thalamic neurons, Taube, 1995), and does not work well for neurons with broad tuning and high baseline firing rates. However, these values are illustrated in Supplementary Figure 2. We examined directional information at the population level by asking whether we could decode the current directional heading from the firing patterns of the neurons using the same approach we used for the spatial decoding described above. We found that although we could decode head direction above chance levels in both regions, decoding was significantly better in the RSC than in the HPC ($t(1998) = 347.98$, $p < .001$, Figure 5g).

Interestingly, RSC directional firing was context dependent. Directional tuning curves were significantly more correlated for visits to the same context than for visits to different contexts (same context $r = .45 \pm 0.02$, between context $r = .23 \pm 0.02$, $t(138) = 9.26$, $p < .001$). Among the 96 neurons with apparent directional tuning in at least one context (see L–N model, next section), 49 (51%) had no directional tuning in the other context. For the remaining neurons that had directional tuning in both contexts ($n = 47$, 49%), we rotated the tuning curves for the black box in 6° increments and correlated them with the tuning curves recorded in the white box in order to determine whether directional preferences rotated with the change in context. We took the rotation with the highest correlation as the amount of rotation observed in response to the context manipulation. Among these neurons, nine neurons showed no rotation (i.e., the maximum correlation was observed at 0° of rotation, Supplementary Figure 2, plot c). Although the remaining 38 neurons could exhibit varying amounts of rotation, a majority of them ($n = 25$) exhibited rotations clustered around 70° clockwise (e.g., Figure 5c, plots 1–2). The reasons for this are uncertain, as the boxes did not rotate and there were no prominent cues that rotated by this amount across the two context conditions. However, it is possible that the neurons were sensitive to one or more distal cues that were visible in one context, but obscured by the curtains in the other context (see Methods, Section 2.2.1). Interestingly, the directional preferences of simultaneously recorded neurons appeared to shift coherently, consistent with previous reports of coherent shifts in anterior dorsal thalamic directional coding (Taube & Burton, 1995). In six recording sessions, we had three or more neurons with directional tuning in both contexts. In four of those sessions, all of the neurons rotated by approximately the same amount (case 1 = 81° ± 3.87; case 2 = 76.5° ± 4.5; case 3 = 69° ± 2.85; case 4 = 68.25° ± 1.86). In one session, all three neurons showed no rotation. In the sixth session, two neurons showed no rotation while two others rotated by 48° and 60°.

3.4 | L–N model

Individual HPC and RSC neurons are known to respond to more than one task variable. For example, HPC neurons are often sensitive to the rat's speed of locomotion in addition to the spatial location (Mcnaughton et al., 1983). To formally assess this, we subjected the open field data from each HPC and RSC neuron to a L–N model (Hardcastle et al., 2017), which generates a firing rate tuning curve for each of the relevant variables and then assesses the significance of each variable as a predictor of neural firing. A key advantage of this approach is that it can identify neurons that are significantly tuned to two or more variables. For this analysis, we used spatial position within the environment, context (black or white box), head direction, running speed, acceleration, and angular velocity as potential predictor variables (Figure 6). Consistent with the above analyses, neurons in both regions were tuned to spatial position and context. Positional tuning was more prevalent in HPC neurons (85% of HPC neurons, compared to 45% of RSC neurons) while contextual tuning was similar in the two regions (58% of HPC neurons, compared to 52% of RSC neurons). Note that tuning to spatial position and context are linked in the HPC, but are more independent in the RSC. This is because all of the HPC neurons that differentiated the black and white contexts had spatial tuning whereas RSC neurons often had a rate code that differentiated the contexts even when there was no spatial tuning. Directional tuning was far more prevalent in the RSC than in the HPC (67% of RSC neurons, compared to 15% of HPC neurons). Among the RSC neurons with directional tuning, about half also showed spatial tuning (see Figure 5a). Conversely, most of the RSC neurons that were tuned to spatial position were also tuned to head direction (51 of the 65 neurons that were significantly tuned to position). This suggests that spatial tuning was typically found in conjunction with directional tuning, but directional tuning could exist independently of spatial tuning in the RSC. In contrast, all of the HPC neurons that showed significant directional tuning (15%, 43/282) also had place fields. Neurons in both regions were sensitive to the rat's running speed, although this was somewhat more prevalent in the RSC (78% compared to 63% in the HPC). A substantial percentage of RSC neurons were also tuned to acceleration (32%) and angular velocity (22%), whereas less than 5% of HPC neurons were tuned to these variables.

FIGURE 5 Directional coding. Plots (a) and (b) show illustrative examples of directional coding in RSC and HPC neurons. For each example, the firing rate in 20° directional bins is illustrated by a circular histogram. Insets illustrating the normalized firing rates (min to max) are also shown to highlight preferred firing direction. Spatial firing rate maps are also shown for each neuron. Plot (c) shows three examples of RSC neurons showing context dependency of directional firing. Plot (d) illustrates the distribution of mutual information between firing rate and head direction for all neurons in each region, while plot (e) illustrates the correlation between directional firing rate histograms during the first and second visit to each context. Plot (f) illustrates the firing rates for RSC and HPC, one neuron per row, with the peak firing aligned to 0° and sorted by the amount of multi-directionality exhibited by each neuron (see text). Plot (g) shows the classification accuracy for decoding the head direction on the basis of the firing rates from neuronal populations in each region. Chance accuracy (5%) is illustrated by the dashed line.

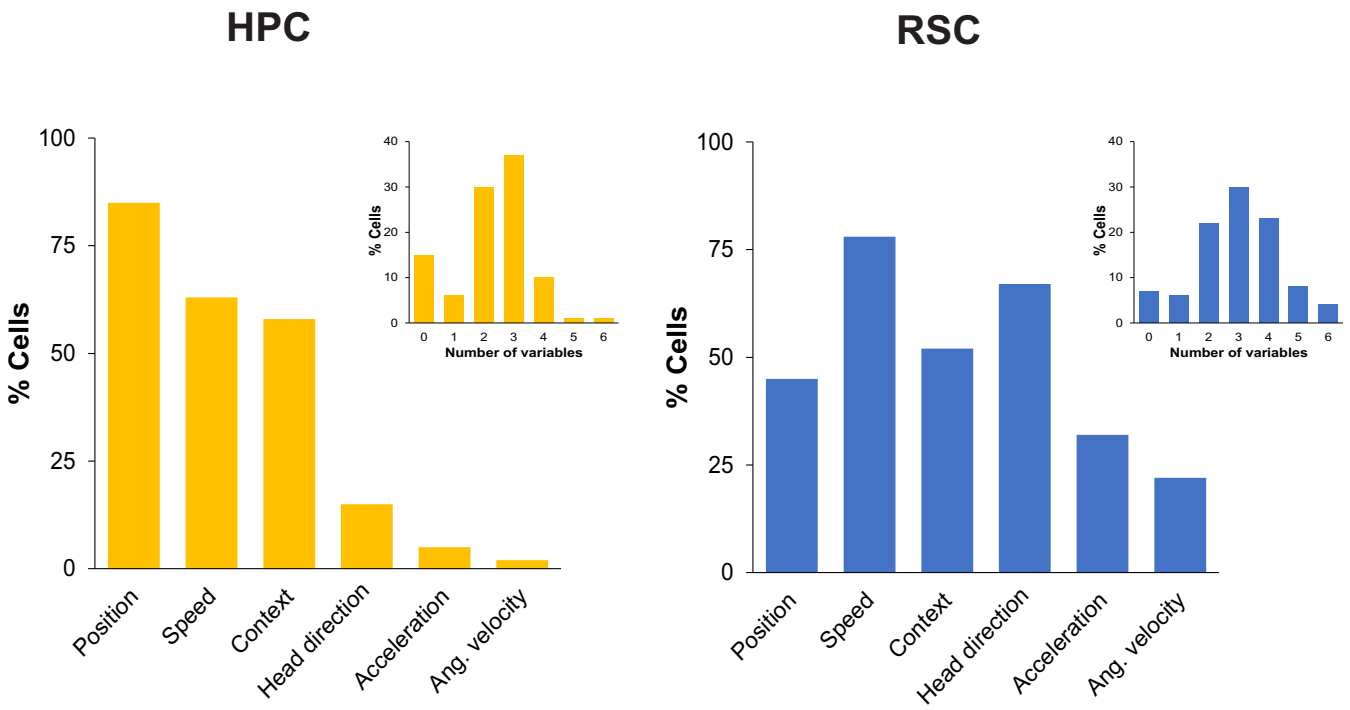

FIGURE 6 Bar plots illustrating the percentage of hippocampus (HPC) and retrosplenial cortex (RSC) neurons that were significantly tuned to each of six behavioral variables, as indicated by an linear–nonlinear (L–N) model analysis (see text). Inset plots illustrate the percentage of neurons with tuning to zero, one, or more variables.

Overall, RSC neurons were more likely to carry information about multiple variables (Figure 6 insets). For example, 65% of RSC neurons were tuned to three or more of the six variables we examined, as compared to 49% of HPC neurons. More strikingly, 35% of RSC neurons were significantly tuned to at least four variables and 12% were tuned to five or six variables, compared to 12% and 2% of HPC neurons, respectively. In the HPC, the encoding of spatial position was clearly dominant. Among the 85% of HPC neurons that had significant tuning to one or more of the six variables, all showed significant tuning to spatial position. That is, although HPC neurons could show tuning to multiple factors, such as the context and running speed, they were always tuned to spatial position. In contrast, RSC tuning typically included a wide range of the variables and combinations of variables. For example, among the RSC neurons with significant tuning to three variables, head direction was a factor 64% of the time, context 52%, spatial position 43%, and running speed 82% of the time.

3.5 | Trajectory and reward location coding

The continuous T-maze affords the opportunity to compare trajectory coding and firing at reward locations in the HPC and RSC (Miller et al., 2019; D. M. Smith et al., 2012; Wood et al., 2000). Neurons in the HPC and RSC exhibited differential firing patterns as the rats traversed the stem of the maze on left and right turn trials, commonly referred to as "splitters" (Figure 7a,b). For each neuron, we compared the firing rates of the left and right trials and computed a *t*-score (Student's *t*) to serve as a measure that incorporates the trial-by-trial reliability of firing differences. The distribution of these values is illustrated in Figure 7c. To examine this at the population level, we computed the Euclidean distance between the population vector for each trial and the average population vector of the left trials and the right trials, leaving out the sample trial. This specificity measure reflects the degree to which the firing pattern on each trial is both similar to other trials of the same type (left or right) and different from trials of the opposite type. For nearly all trials, the population firing pattern was more similar to the same trial type (Figure 7d, dots above the unity line). Interestingly, the first left and first right trials were associated with the highest distance measures (Figure 7d, bold outlined dots), indicating that firing patterns during the initial traversal of the maze differed from those of the later trials. Firing rates were not uniformly higher or lower than average on these initial trials, but were more variable, suggesting that a full circuit of the maze is required before the neurons settle into their typical splitter firing patterns. We also attempted to decode the left or right trials using a minimum distance classifier and found that we could correctly classify the trials more than 89.6% (±0.20) and 83.9% (±0.23) of the time for HPC and RSC, respectively, with HPC accuracy significantly greater than RSC accuracy ($t(1998) = 21.65$, $p < .001$, Figure 7d inset).

We performed a similar analysis on the firing patterns at the time of the reward (Figure 8a,b). Here, for each neuron, we computed a *t*-score comparing the firing rates during the 2 s after arrival at the reward location for the left and right trials. In the RSC, the distribution of *t*-scores was broader, with more values in the tails (Figure 8c),

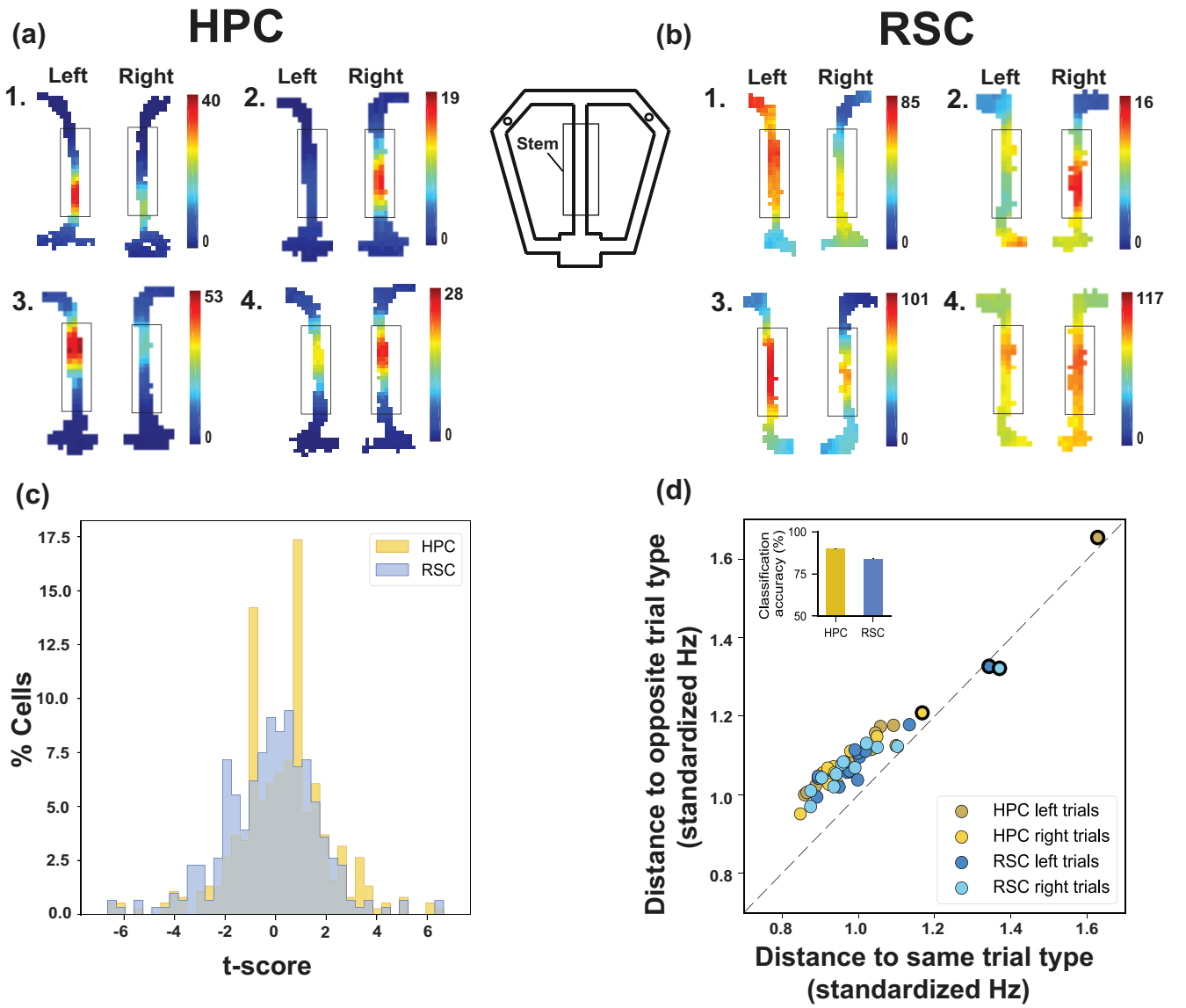

FIGURE 7 Trial-type specific firing on the stem of the T-maze. Plots (a) and (b) show firing rate maps illustrating differential firing during traversals of the central stem of the maze on left and right trials, for example, hippocampus (HPC) and retrosplenial cortex (RSC) neurons. Plot (c) shows the distribution of *t*-scores comparing the firing rates during the left and right trials for each neuron. Plot (d) shows the Euclidean distance between the population vector for each trial (colored dots) and the average population vector of the same and opposite trial types. The highlighted dots with bold outlines illustrate the first left and first right trial. After the initial circuit of the maze, including one left and one right trial, the population firing patterns were always more similar to the current trial type (left or right) than to the opposite trial type, as indicated by dots above the unity line. Classification accuracy for decoding the trial type (left or right) based on the population firing patterns in each region is shown in the inset. Error bars are plotted but are difficult to see, so SEM values are given in the text.

indicating that more of the RSC neurons strongly differentiated the left and right reward locations. Consistent with this, although population firing patterns in both regions exhibited specificity for all trials (greater similarity to the same trial type than to the opposite, Figure 8d), specificity was significantly greater and classification accuracy was significantly higher in the RSC (specificity: $t(40.98) = 14.46$, $p < .001$; classification accuracy: HPC accuracy = 91.97% ± 0.12, RSC accuracy = 99.48% ± 0.02, $t(1998) = 76.35$, $p < .001$, Figure 8d inset).

The rewards serve to motivate task performance, but they also represent an important memory cue since the rats can use the current reward location to predict where the reward will be on the following trial. Therefore, it may be adaptive for neural systems to amplify the differences between the two reward locations. We examined this possibility by asking whether the differentiation was better than would be expected solely on the basis of spatial distance. The reward locations are 105 cm apart on the T-maze, so we estimated the baseline spatial differentiation by computing the Euclidean distance between population vectors for two other, non-reward locations 105 cm apart on opposite sides of the maze (locations on the return arms away from the reward dispenser). We then compared that value to the

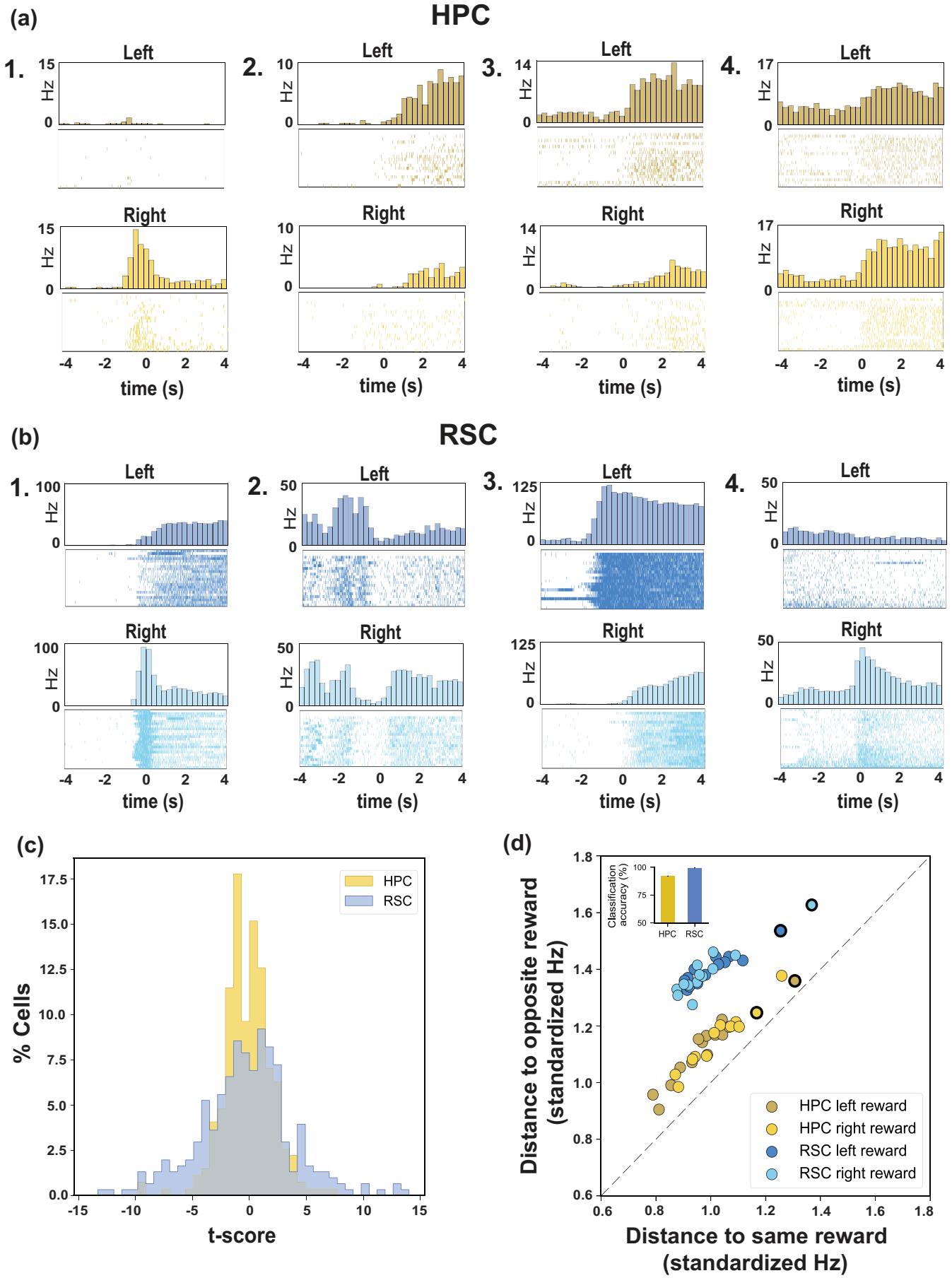

FIGURE 8 Legend on next page.

Euclidean distance between the two reward locations on the maze. We found that RSC neurons differentiated the two reward locations far more than they differentiated equally distant non-reward locations (mean Euclidean distance between reward locations = 0.17, compared to 0.05 for the non-reward locations, $t(50) = 17.39$, $p < .001$), suggesting that the RSC enhances differentiation of the reward locations. In contrast, HPC neurons differentiated the reward locations significantly less than expected on the basis of spatial distance alone (mean Euclidean distance between reward locations = 0.07, compared to 0.11 for the non-reward locations, $t(50) = 4.88$, $p < .001$), possibly because HPC neurons often fired at both reward locations, but rarely had place fields at both of the two non-reward locations used for this comparison. Thus, although neuronal firing patterns in both regions distinguished the left and right reward locations, RSC neurons differentiated them to a greater degree than HPC neurons.

4 | DISCUSSION

Our comparison of HPC and RSC neuronal firing confirmed that these two regions share functional properties, especially a strong tendency to encode spatial and contextual information. Neurons in both regions carry information about the rat's current spatial location and, in the T-maze task, the trajectory through the environment and the locations of rewards. These findings are consistent with the profound spatial navigation deficits that result from either HPC or RSC damage (Holdstock et al., 2000; Ino et al., 2007; Keene & Bucci, 2009; Morris et al., 1982; Spiers et al., 2001; Takahashi et al., 1997). Neurons in both regions also clearly discriminate between environmental contexts. This is particularly important because contextual memory links spatial cognition to broader memory functions. Memories are linked to the context where they were acquired and the context is, itself, a powerful retrieval cue. Thus, neural representations of the context are critical for a wide variety of memories, from conditioned responses (J. J. Kim & Fanselow, 1992; Penick & Solomon, 1991) to episodic memory (S. M. Smith, 1979, 1988; for review see D. M. Smith, 2008), and, like spatial memory, contextual memory is severely impaired by lesions of the HPC or RSC (Butterly et al., 2012; Cowansage et al., 2014; Keene & Bucci, 2008; J. J. Kim & Fanselow, 1992). We have found that a key benefit of creating distinct representations of different contexts is that it allows for the retrieval of situationally relevant memories while simultaneously preventing interference from irrelevant memories (Bulkin et al., 2016; D. M. Smith & Bulkin, 2014). These similarities are consistent with the idea that the HPC and RSC are two components of a functional circuit that mediates spatial cognition and memory (Alexander et al., 2018; Alexander, Robinson, et al., 2020; Miller et al., 2014; D. M. Smith et al., 2022; Vann et al., 2009).

Despite these similarities, our results also identify a number of key differences between the two regions which suggest that they may make distinct contributions and employ different coding schemes. Neurons in both regions carried information about the rat's current spatial location, but this coding was more prominent in the HPC. Consistent with expectations, most HPC neurons exhibited clear well-defined place fields and we could decode the rat's current location from population firing patterns in the HPC better than we could in the RSC. Neurons in both regions frequently encoded more than one task variable, such as context, running speed, and head direction. However, spatial location was nearly always a significant factor in the HPC whereas spatial location was only a significant factor for about half of RSC neurons. Although both regions clearly differentiated the two environmental contexts using both a spatial code and a rate code, the balance of these two coding strategies differed. The HPC produced a stronger spatial code while the RSC produced a stronger rate code. These findings are consistent with the idea that an obligatory neural code for spatial location is at the center of HPC representations, at least in these two experimental tasks which are optimized for examining spatial and contextual representations. In contrast, while spatial location is a prominent component of RSC representations, other task variables may be equally prominent. For example, head direction and context were also prominent in RSC representations, and both could be expressed independent of spatial location in the RSC. Differences were also found in the T-maze task. Consistent with previous reports (Miller et al., 2019; D. M. Smith & Mizumori, 2006; Wood et al., 2000), neurons in both regions exhibited differential firing on the stem of the T-maze (i.e. splitter firing) and at the reward locations. However, splitter firing was more distinct in the HPC, whereas encoding of the reward location was better in the RSC. RSC neurons were also more sensitive to movement variables. Although neurons in both regions were tuned to running speed, only the RSC has a substantial proportion of neurons significantly tuned to angular velocity and acceleration (see also Cho & Sharp, 2001).

The most striking difference was that information about head direction was prominent in the RSC, but only weakly encoded in the

FIGURE 8 Reward location-specific firing on the T-maze. Plots (a) and (b) show peri-event time histograms with spike rasters centered on the time of arrival at the reward location (time zero) for example hippocampus (HPC) and retrosplenial cortex (RSC) neurons. Data for left and right reward locations are plotted separately for each neuron. Plot (c) shows the distribution of *t*-scores comparing the firing rates during the 2 s after arrival at the reward for left and right trials for each neuron. Note that the RSC distribution has more values at the extremes, compared to the HPC, with negative values indicating greater firing at the right reward and positive values indicating greater firing at the left reward location. Plot (d) shows the Euclidean distance between the population vector for each trial (colored dots) and the average population vector of the same and opposite reward locations. Note that RSC population firing patterns are farther from the unity line than HPC neurons, indicating greater reward location specificity in the RSC. As in Figure 7, the first left and first right rewards are indicated by highlighted dots (bold outlines). Classification accuracy for decoding the left or right reward location based on the population firing patterns in each region is shown in the inset. Error bars are plotted but are difficult to see, so SEM values are given in the text.

HPC. This difference is likely due to the dense interconnection between the RSC and the anterior dorsal thalamus, which is a key component of the head direction system (Taube, 1995), although the postrhinal and parietal cortex may also provide directional input (LaChance et al., 2022; Wilber et al., 2014). To the extent that directional firing is linked to visual landmarks, input from the visual system may also be important (Powell et al., 2020; Sit & Goard, 2023; Zhang et al., 2022). In the RSC, directional firing was the most frequently identified correlate, other than running speed, and it could occur in conjunction with spatially localized firing or in neurons with no clear spatial specificity. We found that neurons could have a single preferred direction or multiple peaks in the directional tuning curve and these preferred directions often aligned with the geometry of the environment. These results are broadly consistent with previous findings of double or quadruple-peaked tuning curves in environments with two or four different compartments arranged to form a symmetrical environment (Jacob et al., 2017; Zhang et al., 2022). However, where the previous studies found relatively specific, high contrast tuning curves in a small subset of RSC neurons, we found that more than half of our neurons exhibited significant directional tuning with broad tuning curves and high background firing rates. The directional tuning we observed was reliable across repeated passes through the various directional headings and across repeated visits to the same environment. Moreover, we could readily predict the rat's current head direction from population firing patterns. It is not clear whether the apparent differences between our findings and the previous studies result from the relatively strict classification criteria used in the previous studies or, more intriguingly, whether RSC directional tuning is sharpened by exposure to environments defined by symmetrical compartments that are highly salient but challenging to discriminate. The latter possibility is consistent with the observation that RSC neurons flexibly respond to a wide variety of cues and environmental features (D. M. Smith et al., 2018).

Our observations suggest that the HPC and RSC use different representational schemes even when they carry similar kinds of information. For example, although neurons in both regions carry information about the rat's current spatial location, HPC neurons exhibited the expected small, circumscribed, high-contrast place fields, consistent with a sparse coding mechanism (Beyeler et al., 2019; Rolls & Treves, 1990; Skaggs & McNaughton, 1992). In contrast, RSC neurons had high baseline firing rates and they generally did not exhibit true place fields. Instead, their firing rate varied reliably across wide areas of the environment, which is more consistent with a distributed coding mechanism. Similarly broad spatial firing patterns are seen in the subiculum and spatial coding becomes progressively more distributed with increasing distance from CA1, but subicular neurons nevertheless exhibit good spatial coding (S. M. Kim et al., 2012). This is notable given that the subiculum is the main source of hippocampal system output to the RSC (Van Groen & Wyss, 2003). We did see a few cases where RSC neurons showed more constrained spatial firing patterns on the T-maze, but it is difficult to rule out the influence of movement variables and heading direction. The same pattern of broad tuning and high background firing was also apparent in RSC directional firing.

Sparse and distributed coding schemes also influence the manner in which these two regions make use of spatial representations to differentiate environmental contexts. As expected, HPC neurons exhibited global remapping with most neurons having place fields in one environment, but not the other. In cases where the neurons had place fields in both contexts, the preferred firing locations were unrelated. This resulted in spatial firing patterns that were nearly fully orthogonalized in the two contexts (Figure 1a). This combination of sparse coding and orthogonalization means that a large number of contexts can be efficiently differentiated (Alme et al., 2014), and this is a key characteristic that underpins theoretical accounts of the HPC role in contextual memory (Kubie et al., 2020; Nadel, 2008; D. M. Smith & Bulkin, 2014). RSC spatial firing patterns were not orthogonalized. Instead, RSC representations of different contexts had enough overlap that it was possible to use the firing map from one context to predict the rat's location in the other context well above chance levels. Nevertheless, RSC spatial firing patterns did reliably differentiate contexts because most neurons fired more similarly during trials in the same context than for trials in different contexts (Figure 3b). Each RSC neuron contributed only a little information to the overall differentiation of the two contexts, consistent with a distributed population code, and the overall firing patterns could support generalization across contexts. One interesting departure from this orthogonalization versus generalization result is the encoding of reward locations. RSC neurons were better at differentiating the reward locations than HPC neurons, possibly related to the RSC role in stimulus discrimination tasks (Gabriel, 1993; D. M. Smith et al., 2018).

Another characteristic of distributed coding is that individual neurons may carry information about more than one stimulus or task variable, referred to as multiplexing or mixed selectivity (Fusi et al., 2016; Hardcastle et al., 2017; Meister et al., 2013; Rigotti et al., 2013). Although present in both regions, multiplexing was more prevalent in the RSC. Most RSC neurons were tuned to several of the variables we examined using the L–N model. For example, neurons that were tuned to head direction and spatial location can be seen in Figure 5a, plots 4–6. Although we did not formally assess multiplexing in the T-maze task, we observed many examples of neurons that showed splitter firing, along with preferential firing at one of the reward sites or other locations (see also Vedder et al., 2017). Our analysis of RSC multiplexing was constrained by the fact that the open field task offers a limited number of variables for assessment, but more complex tasks with more variables could reveal even greater RSC multiplexing. For example, previous studies have shown that RSC neurons can also incorporate visual and auditory information as well as the valence of conditioning cues into their firing patterns (Fischer et al., 2020; D. M. Smith et al., 2001, 2004, 2018; Vedder et al., 2017), suggesting that the RSC is capable of integrating a wide array of inputs, depending on the task demands. This tendency to incorporate a wide range of variables may contribute to the array of idiosyncratic RSC spatial firing patterns we observed. HPC neurons also showed tuning to multiple variables, but it was more constrained. Fewer HPC neurons had tuning to three or more variables as compared to the RSC and, as mentioned above, spatial location was nearly always the dominant factor in the HPC.

Overall, our results emphasize the shared functional characteristics of the HPC and RSC, but they also illustrate some key differences in their contributions to spatial and contextual memory. Moreover, these two regions employ different representational schemes, with highly orthogonalized sparse representations in the HPC and distributed multiplexed representations in the RSC. A growing body of evidence suggests that HPC representations are consolidated into the RSC (Alexander et al., 2018; Cowansage et al., 2014; De Sousa et al., 2019; Katche et al., 2013; Mao et al., 2018; Milczarek et al., 2018). Our results are consistent with the idea that the consolidation process may result in more distributed representations that can support generalization (McClelland et al., 1995; Sun et al., 2023). However, RSC representations were not simply a cortical copy of the HPC representations. The RSC encoded information about head direction, presumably resulting from communication via the dense interconnections with the anterior thalamus (Bubb et al., 2017; Van Groen, 1993; Van Groen & Wyss, 2003). Other RSC firing patterns, such as border and corner firing (Figure 1b) may result from interactions with the entorhinal cortex, where border firing has been observed (Solstad et al., 2008). Similarly, the sensitivity of RSC neurons to movement variables and route segments such as turns may reflect input from the parietal cortex (Alexander, Place, et al., 2023; Clark et al., 2018). The inputs that contribute to rate coding of the context in RSC neurons are not known, but given that the color of the environment (black or white) was a prominent characteristic of the two contexts, it is likely that visual input is critical (Fischer et al., 2020; Mao et al., 2020; Powell et al., 2020). These considerations suggest that the RSC generates representations that integrate information from a variety of inputs, including but not limited to the HPC.

ACKNOWLEDGMENT

This work was supported by MH083809 to D. Smith.

DATA AVAILABILITY STATEMENT

The data that support the findings of this study are available from the corresponding author upon reasonable request.

ORCID

Dev Laxman Subramanian https://orcid.org/0000-0002-2019-264X
David M. Smith https://orcid.org/0000-0002-5156-8099

REFERENCES

Alexander, A. S., Carstensen, L. C., Hinman, J. R., Raudies, F., Chapman, G. W., & Hasselmo, M. E. (2020). Egocentric boundary vector tuning of the retrosplenial cortex. *Science Advances*, *6*(8), eaaz2322. https://doi.org/10.1126/sciadv.aaz2322

Alexander, A. S., & Nitz, D. A. (2015). Retrosplenial cortex maps the conjunction of internal and external spaces. *Nature Neuroscience*, *18*(8), 1143–1151. https://doi.org/10.1038/nn.4058

Alexander, A. S., & Nitz, D. A. (2017). Spatially periodic activation patterns of retrosplenial cortex encode route sub-spaces and distance traveled. *Current Biology*, *27*(11), 1551–1560.e4. https://doi.org/10.1016/j.cub.2017.04.036

Alexander, A. S., Place, R., Starrett, M. J., Chrastil, E. R., & Nitz, D. A. (2023). Rethinking retrosplenial cortex: Perspectives and predictions. *Neuron*, *111*(2), 150–175. https://doi.org/10.1016/J.NEURON.2022.11.006

Alexander, A. S., Rangel, L. M., Tingley, D., & Nitz, D. A. (2018). Neurophysiological signatures of temporal coordination between retrosplenial cortex and the hippocampal formation. *Behavioral Neuroscience*, *132*(5), 453–468. https://doi.org/10.1037/bne0000254

Alexander, A. S., Robinson, J. C., Dannenberg, H., Kinsky, N. R., Levy, S. J., Mau, W., Chapman, G. W., Sullivan, D. W., & Hasselmo, M. E. (2020). Neurophysiological coding of space and time in the hippocampus, entorhinal cortex, and retrosplenial cortex. *Brain and Neuroscience Advances*, *4*, 239821282097287. https://doi.org/10.1177/2398212820972871

Alexander, A. S., Robinson, J. C., Stern, C. E., & Hasselmo, M. E. (2023). Gated transformations from egocentric to allocentric reference frames involving retrosplenial cortex, entorhinal cortex, and hippocampus. *Hippocampus*, *33*(5), 465–487. https://doi.org/10.1002/HIPO.23513

Alme, C. B., Miao, C., Jezek, K., Treves, A., Moser, E. I., & Moser, M. B. (2014). Place cells in the hippocampus: Eleven maps for eleven rooms. *Proceedings of the National Academy of Sciences of the United States of America*, *111*(52), 18428–18435. https://doi.org/10.1073/pnas.1421056111

Bannerman, D. M., Yee, B. K., Lemaire, M., Wilbrecht, L., Jarrard, L., Iversen, S. D., Rawlins, J. N. P., & Good, M. A. (2001). The role of the entorhinal cortex in two forms of spatial learning and memory. *Experimental Brain Research*, *141*(3), 281–303. https://doi.org/10.1007/S002210100868

Beyeler, M., Rounds, E. L., Carlson, K. D., Dutt, N., & Krichmar, J. L. (2019). Neural correlates of sparse coding and dimensionality reduction. *PLoS Computational Biology*, *15*(6), e1006908. https://doi.org/10.1371/JOURNAL.PCBI.1006908

Brennan, E. K. W., Sudhakar, S. K., Jedrasiak-Cape, I., John, T. T., & Ahmed, O. J. (2020). Hyperexcitable neurons enable precise and persistent information encoding in the superficial retrosplenial cortex. *Cell Reports*, *30*(5), 1598–1612.e8. https://doi.org/10.1016/j.celrep.2019.12.093

Bubb, E. J., Kinnavane, L., & Aggleton, J. P. (2017). Hippocampal–diencephalic–cingulate networks for memory and emotion: An anatomical guide. *Brain and Neuroscience Advances*, *1*, 239821281772344. https://doi.org/10.1177/2398212817723443

Bulkin, D. A., Law, L. M., & Smith, D. M. (2016). Placing memories in context: Hippocampal representations promote retrieval of appropriate memories. *Hippocampus*, *26*(7), 958–971. https://doi.org/10.1002/hipo.22579

Butterly, D. A., Petroccione, M. A., & Smith, D. M. (2012). Hippocampal context processing is critical for interference free recall of odor memories in rats. *Hippocampus*, *22*(4), 906–913. https://doi.org/10.1002/hipo.20953

Carstensen, L. C., Alexander, A. S., Chapman, G. W., Lee, A. J., & Hasselmo, M. E. (2021). Neural responses in retrosplenial cortex associated with environmental alterations. *IScience*, *24*(11), 103377. https://doi.org/10.1016/J.ISCI.2021.103377

Cho, J., & Sharp, P. E. (2001). Head direction, place, and movement correlates for cells in the rat retrosplenial cortex. *Behavioral Neuroscience*, *115*(1), 3–25. https://doi.org/10.1037/0735-7044.115.1.3

Clark, B. J., & Harvey, R. E. (2016). Do the anterior and lateral thalamic nuclei make distinct contributions to spatial representation and memory? In *Neurobiology of learning and memory* (Vol. 133, pp. 69–78). Academic Press. https://doi.org/10.1016/j.nlm.2016.06.002

Clark, B. J., Simmons, C. M., Berkowitz, L. E., & Wilber, A. A. (2018). The retrosplenial-parietal network and reference frame coordination for spatial navigation. *Behavioral Neuroscience*, *132*(5), 416–429. https://doi.org/10.1037/bne0000260

Cowansage, K. K., Shuman, T., Dillingham, B. C., Chang, A., Golshani, P., & Mayford, M. (2014). Direct reactivation of a coherent neocortical memory of context. *Neuron*, *84*, 432–441. https://doi.org/10.1016/j.neuron.2014.09.022

De Sousa, A. F., Cowansage, K. K., Zutshi, I., Cardozo, L. M., Yoo, E. J., Leutgeb, S., & Mayford, M. (2019). Optogenetic reactivation of memory ensembles in the retrosplenial cortex induces systems consolidation. *Proceedings of the National Academy of Sciences of the United States of America*, *116*(17), 8576–8581. https://doi.org/10.1073/PNAS.1818432116

Fischer, L. F., Mojica Soto-Albors, R., Buck, F., & Harnett, M. T. (2020). Representation of visual landmarks in retrosplenial cortex. *eLife*, *9*, e51458. https://doi.org/10.7554/eLife.51458

Fournier, D. I., Cheng, H. Y., Robinson, S., & Todd, T. P. (2021). Cortical contributions to higher-order conditioning: A review of retrosplenial cortex function. *Frontiers in Behavioral Neuroscience*, *15*, 682426. https://doi.org/10.3389/FNBEH.2021.682426

Fournier, D. I., Monasch, R. R., Bucci, D. J., & Todd, T. P. (2020). Retrosplenial cortex damage impairs unimodal sensory preconditioning. *Behavioral Neuroscience*, *134*(3), 198–207. https://doi.org/10.1037/BNE0000365

Fox, S. E., & Ranck, J. B. (1981). Electrophysiological characteristics of hippocampal complex-spike cells and theta cells. *Experimental Brain Research*, *41*(3–4), 399–410. https://doi.org/10.1007/BF00238898

Frank, L. M., Brown, E. N., & Wilson, M. A. (2001). A comparison of the firing properties of putative excitatory and inhibitory neurons from CA1 and the entorhinal cortex. *Journal of Neurophysiology*, *86*(4), 2029–2040. https://doi.org/10.1152/JN.2001.86.4.2029

Fusi, S., Miller, E. K., & Rigotti, M. (2016). Why neurons mix: High dimensionality for higher cognition. *Current Opinion in Neurobiology*, *37*, 66–74. https://doi.org/10.1016/J.CONB.2016.01.010

Gabriel, M. (1993). Discriminative avoidance learning: A model system. In B. A. Vogt & M. Gabriel (Eds.), *Neurobiology of cingulate cortex and limbic thalamus* (pp. 478–523). Birkhauser.

Hafting, T., Fyhn, M., Molden, S., Moser, M. B., & Moser, E. I. (2005). Microstructure of a spatial map in the entorhinal cortex. *Nature*, *436*(7052), 801–806. https://doi.org/10.1038/NATURE03721

Hardcastle, K., Maheswaranathan, N., Ganguli, S., & Giocomo, L. M. (2017). A multiplexed, heterogeneous, and adaptive code for navigation in medial entorhinal cortex. *Neuron*, *94*(2), 375–387.e7. https://doi.org/10.1016/J.NEURON.2017.03.025

Holdstock, J. S., Mayes, A. R., Cezayirli, E., Isaac, C. L., Aggleton, J. P., & Roberts, N. (2000). A comparison of egocentric and allocentric spatial memory in a patient with selective hippocampal damage. *Neuropsychologia*, *38*(4), 410–425. https://doi.org/10.1016/S0028-3932(99)00099-8

Ino, T., Doi, T., Hirose, S., Kimura, T., Ito, J., & Fukuyama, H. (2007). Directional disorientation following left retrosplenial hemorrhage: A case report with FMRI studies. *Cortex*, *43*(2), 248–254. https://doi.org/10.1016/S0010-9452(08)70479-9

Jacob, P. Y., Casali, G., Spieser, L., Page, H., Overington, D., & Jeffery, K. (2017). An independent, landmark-dominated head-direction signal in dysgranular retrosplenial cortex. *Nature Neuroscience*, *20*(2), 173–175. https://doi.org/10.1038/nn.4465

Jankowski, M. M., Passecker, J., Islam, M. N., Vann, S., Erichsen, J. T., Aggleton, J. P., & O'Mara, S. M. (2015). Evidence for spatially-responsive neurons in the rostral thalamus. *Frontiers in Behavioral Neuroscience*, *9*, 256. https://doi.org/10.3389/fnbeh.2015.00256

Jercog, P. E., Ahmadian, Y., Woodruff, C., Deb-Sen, R., Abbott, L. F., & Kandel, E. R. (2019). Heading direction with respect to a reference point modulates place-cell activity. *Nature Communications*, *10*(1), 2333. https://doi.org/10.1038/S41467-019-10139-7

Katche, C., Dorman, G., Gonzalez, C., Kramar, C. P., Slipczuk, L., Rossato, J. I., Cammarota, M., & Medina, J. H. (2013). On the role of retrosplenial cortex in long-lasting memory storage. *Hippocampus*, *23*(4), 295–302. https://doi.org/10.1002/hipo.22092

Keene, C. S., & Bucci, D. J. (2008). Neurotoxic lesions of retrosplenial cortex disrupt signaled and unsignaled contextual fear conditioning. *Behavioral Neuroscience*, *122*(5), 1070–1077. https://doi.org/10.1037/a0012895

Keene, C. S., & Bucci, D. J. (2009). Damage to the retrosplenial cortex produces specific impairments in spatial working memory. *Neurobiology of Learning and Memory*, *91*(4), 408–414. https://doi.org/10.1016/J.NLM.2008.10.009

Kim, J. J., & Fanselow, M. S. (1992). Modality-specific retrograde amnesia of fear. *Science*, *256*(5057), 675–677. https://doi.org/10.1126/science.1585183

Kim, S. M., Ganguli, S., & Frank, L. M. (2012). Spatial information outflow from the hippocampal circuit: Distributed spatial coding and phase precession in the subiculum. *Journal of Neuroscience*, *32*(34), 11539–11558. https://doi.org/10.1523/JNEUROSCI.5942-11.2012

Kubie, J. L., Levy, E. R. J., & Fenton, A. A. (2020). Is hippocampal remapping the physiological basis for context? *Hippocampus*, *30*(8), 851–864. https://doi.org/10.1002/HIPO.23160

Kubie, J. L., Muller, R. U., & Bostock, E. (1990). Spatial firing properties of hippocampal theta cells. *The Journal of Neuroscience*, *10*(4), 1110–1123. https://doi.org/10.1523/JNEUROSCI.10-04-01110.1990

LaChance, P. A., Graham, J., Shapiro, B. L., Morris, A. J., & Taube, J. S. (2022). Landmark-modulated directional coding in postrhinal cortex. *Science Advances*, *8*(4), 8404. https://doi.org/10.1126/SCIADV.ABG8404

Law, L. M., Bulkin, D. A., & Smith, D. M. (2016). Slow stabilization of concurrently acquired hippocampal context representations. *Hippocampus*, *26*(12), 1560–1569. https://doi.org/10.1002/hipo.22656

Leutgeb, S., Ragozzino, K. E., & Mizumori, S. J. Y. (2000). Convergence of head direction and place information in the CA1 region of hippocampus. *Neuroscience*, *100*(1), 11–19. https://doi.org/10.1016/S0306-4522(00)00258-X

Leutgeb, S., Leutgeb, J. K., Barnes, C. A., Moser, E. I., McNaughton, B. L., & Moser, M. B. (2005). Independent codes for spatial and episodic memory in hippocampal neuronal ensembles. *Science*, *309*(5734), 619–623. https://doi.org/10.1126/SCIENCE.1114037

Mair, R. G. (1994). On the role of thalamic pathology in diencephalic amnesia. *Reviews in the Neurosciences*, *5*(2), 105–140. https://doi.org/10.1515/REVNEURO.1994.5.2.105

Mao, D., Molina, L. A., Bonin, V., & McNaughton, B. L. (2020). Vision and locomotion combine to drive path integration sequences in mouse retrosplenial cortex. *Current Biology*, *30*(9), 1680–1688.e4. https://doi.org/10.1016/J.CUB.2020.02.070

Mao, D., Neumann, A. R., Sun, J., Bonin, V., Mohajerani, M. H., & McNaughton, B. L. (2018). Hippocampus-dependent emergence of spatial sequence coding in retrosplenial cortex. *Proceedings of the National Academy of Sciences of the United States of America*, *115*(31), 8015–8018. https://doi.org/10.1073/pnas.1803224115

Markus, E. J., Barnes, C. A., McNaughton, B. L., Gladden, V. L., & Skaggs, W. E. (1994). Spatial information content and reliability of hippocampal CA1 neurons: Effects of visual input. *Hippocampus*, *4*(4), 410–421. https://doi.org/10.1002/hipo.450040404

McClelland, J. L., McNaughton, B. L., & O'Reilly, R. C. (1995). Why there are complementary learning systems in the hippocampus and neocortex: Insights from the successes and failures of connectionist models of learning and memory. *Psychological Review*, *102*(3), 419–457. https://doi.org/10.1037/0033-295X.102.3.419

Mcnaughton, B. L., Barnes, C. A., & O'keefe, J. (1983). The contributions of position, direction, and velocity to single unit activity in the hippocampus of freely-moving rats. *Experimental Brain Research*, *52*, 41–49. https://doi.org/10.1007/bf00237147

Meister, M. L. R., Hennig, J. A., & Huk, A. C. (2013). Signal multiplexing and single-neuron computations in lateral intraparietal area during decision-making. *The Journal of Neuroscience*, *33*(6), 2254–2267. https://doi.org/10.1523/JNEUROSCI.2984-12.2013

Milczarek, M. M., Vann, S. D., & Sengpiel, F. (2018). Spatial memory engram in the mouse retrosplenial cortex. *Current Biology*, *28*, 1975–1980.e6. https://doi.org/10.1016/j.cub.2018.05.002

Miller, A. M. P., Mau, W., & Smith, D. M. (2019). Retrosplenial cortical representations of space and future goal locations develop with learning.

Current Biology, *29*(12), 2083–2090.e4. https://doi.org/10.1016/j.cub.2019.05.034

Miller, A. M. P., Serrichio, A. C., & Smith, D. M. (2021). Dual-factor representation of the environmental context in the retrosplenial cortex. *Cerebral Cortex*, *31*(5), 2720–2728. https://doi.org/10.1093/CERCOR/BHAA386

Miller, A. M. P., Vedder, L. C., Law, L. M., & Smith, D. M. (2014). Cues, context, and long-term memory: The role of the retrosplenial cortex in spatial cognition. *Frontiers in Human Neuroscience*, *8*(August), 1–15. https://doi.org/10.3389/fnhum.2014.00586

Morris, R. G. M., Garrud, P., Rawlins, J. N. P., & O'Keefe, J. (1982). Place navigation impaired in rats with hippocampal lesions. *Nature*, *297*(5868), 681–683. https://doi.org/10.1038/297681a0

Nadel, L. (2008). The hippocampus and context revisited. In S. J. Y. Mizumori (Ed.), *Hippocampal place fields: Relevance to learning and memory* (pp. 3–15). Oxford University Press. https://doi.org/10.1093/ACPROF:OSO/9780195323245.003.0002

O'Keefe, J., & Dostrovsky, J. (1971). The hippocampus as a spatial map. Preliminary evidence from unit activity in the freely-moving rat. *Brain Research*, *34*(1), 171–175. https://doi.org/10.1016/0006-8993(71)90358-1

Olypher, A. V., Lánský, P., Muller, R. U., & Fenton, A. A. (2003). Quantifying location-specific information in the discharge of rat hippocampal place cells. *Journal of Neuroscience Methods*, *127*(2), 123–135. https://doi.org/10.1016/S0165-0270(03)00123-7

Paxinos, G., & Watson, C. (1998). *The rat brain in stereotaxic coordinates*. Academic Press.

Penick, S., & Solomon, P. R. (1991). Hippocampus, context, and conditioning. *Behavioral Neuroscience*, *105*(5), 611–617. https://doi.org/10.1037/0735-7044.105.5.611

Powell, A., Connelly, W. M., Vasalauskaite, A., Nelson, A. J. D., Vann, S. D., Aggleton, J. P., Sengpiel, F., & Ranson, A. (2020). Stable encoding of visual cues in the mouse retrosplenial cortex. *Cerebral Cortex*, *30*(8), 4424–4437. https://doi.org/10.1093/CERCOR/BHAA030

Rigotti, M., Barak, O., Warden, M. R., Wang, X. J., Daw, N. D., Miller, E. K., & Fusi, S. (2013). The importance of mixed selectivity in complex cognitive tasks. *Nature*, *497*(7451), 585–590. https://doi.org/10.1038/nature12160

Robinson, S., Keene, C. S., Iaccarino, H. F., Duan, D., & Bucci, D. J. (2011). Involvement of retrosplenial cortex in forming associations between multiple sensory stimuli. *Behavioral Neuroscience*, *125*(4), 578–587. https://doi.org/10.1037/a0024262

Robinson, S., Todd, T. P., Pasternak, A. R., Luikart, B. W., Skelton, P. D., Urban, D. J., & Bucci, D. J. (2014). Chemogenetic silencing of neurons in retrosplenial cortex disrupts sensory preconditioning. *Journal of Neuroscience*, *34*(33), 10982–10988. https://doi.org/10.1523/JNEUROSCI.1349-14.2014

Rolls, E., & Treves, A. (1990). The relative advantages of sparse versus distributed encoding for associative neuronal networks in the brain. *Network: Computation in Neural Systems*, *1*(4), 407–421. https://doi.org/10.1088/0954-898X/1/4/002

Scoville, W. B., & Milner, B. (1957). Loss of recent memory after bilateral hippocampal lesions. *Journal of Neurology, Neurosurgery, and Psychiatry*, *20*(1), 11–21. https://doi.org/10.1136/jnnp.20.1.11

Sit, K. K., & Goard, M. J. (2023). Coregistration of heading to visual cues in retrosplenial cortex. *Nature Communications*, *14*(1), 1992. https://doi.org/10.1038/S41467-023-37704-5

Skaggs, W. E., & McNaughton, B. L. (1992). Computational approaches to hippocampal function. *Current Opinion in Neurobiology*, *2*(2), 209–211. https://doi.org/10.1016/0959-4388(92)90014-C

Skaggs, W. E., McNaughton, B. L., Gothard, K. M., & Markus, E. (1993). *An information theoretic approach to deciphering the neural code* (pp. 1030–1037). Morgan Kaufmann.

Smith, D. M. (2008). The hippocampus, context processing and episodic memory. In A. E. L. N. Ekrem Dere & P. H. Joseph (Eds.), *Handbook of behavioral neuroscience* (Vol. 18, pp. 465–630). Elsevier. https://doi.org/10.1016/S1569-7339(08)00225-7

Smith, D. M., Barredo, J., & Mizumori, S. J. Y. (2012). Complimentary roles of the hippocampus and retrosplenial cortex in behavioral context discrimination. *Hippocampus*, *22*(5), 1121–1133. https://doi.org/10.1002/hipo.20958

Smith, D. M., & Bulkin, D. A. (2014). The form and function of hippocampal context representations. *Neuroscience and Biobehavioral Reviews*, *40*, 52–61. https://doi.org/10.1016/j.neubiorev.2014.01.005

Smith, D. M., Miller, A. M. P., & Vedder, L. C. (2018). The retrosplenial cortical role in encoding behaviorally significant cues. *Behavioral Neuroscience*, *132*(5), 356–365. https://doi.org/10.1037/bne0000257

Smith, D. M., & Mizumori, S. J. Y. (2006). Learning-related development of context-specific neuronal responses to places and events: The hippocampal role in context processing. *The Journal of Neuroscience*, *26*(12), 3154–3163. https://doi.org/10.1523/JNEUROSCI.3234-05.2006

Smith, D. M., Monteverde, J., Schwartz, E., Freeman, J. H., & Gabriel, M. (2001). Lesions in the central nucleus of the amygdala: Discriminative avoidance learning, discriminative approach learning, and cingulothalamic training-induced neuronal activity. *Neurobiology of Learning and Memory*, *76*, 403–425. https://doi.org/10.1006/nlme.2001.4019

Smith, D. M., Wakeman, D., Patel, J., & Gabriel, M. (2004). Fornix lesions impair context-related cingulothalamic neuronal patterns and concurrent discrimination learning in rabbits (*Oryctolagus cuniculus*). *Behavioral Neuroscience*, *118*(6), 1225–1239. https://doi.org/10.1037/0735-7044.118.6.1225

Smith, D. M., Yang, Y. Y., Subramanian, D. L., Miller, A. M. P., Bulkin, D. A., & Law, L. M. (2022). The limbic memory circuit and the neural basis of contextual memory. *Neurobiology of Learning and Memory*, *187*, 107557. https://doi.org/10.1016/J.NLM.2021.107557

Smith, S. M. (1988). Environmental context-dependent memory. In G. Davies & D. M. Thomson (Eds.), *Memory in context: Context in memory* (pp. 13–34). John Wiley and Sons.

Smith, S. M. (1979). Remembering in and out of context. *Journal of Experimental Psychology: Human Learning and Memory*, *5*(5), 460–471. https://doi.org/10.1037/0278-7393.5.5.460

Solstad, T., Boccara, C. N., Kropff, E., Moser, M. B., & Moser, E. I. (2008). Representation of geometric borders in the entorhinal cortex. *Science*, *322*(5909), 1865–1868. https://doi.org/10.1126/SCIENCE.1166466

Spiers, H. J., Burgess, N., Hartley, T., Vargha-Khadem, F., & O'Keefe, J. (2001). Bilateral hippocampal pathology impairs topographical and episodic memory but not visual pattern matching. *Hippocampus*, *11*(6), 715–725. https://doi.org/10.1002/HIPO.1087

Sugar, J., Witter, M. P., van Strien, N. M., & Cappaert, N. L. M. (2011). The retrosplenial cortex: Intrinsic connectivity and connections with the (para)hippocampal region in the rat. An interactive connectome. *Frontiers in Neuroinformatics*, *5*(July), 1–13. https://doi.org/10.3389/fninf.2011.00007

Sun, W., Advani, M., Spruston, N., Saxe, A., & Fitzgerald, J. E. (2023). Organizing memories for generalization in complementary learning systems. *Nature Neuroscience*, *26*(8), 1438–1448. https://doi.org/10.1038/s41593-023-01382-9

Takahashi, N., Kawamura, M., Shiota, J., Kasahata, N., & Hirayama, K. (1997). Pure topographic disorientation due to right retrosplenial lesion. *Neurology*, *49*(2), 464–469. https://doi.org/10.1212/WNL.49.2.464

Taube, J. S. (1995). Head direction cells recorded in the anterior thalamic nuclei of freely moving rats. *Journal of Neuroscience*, *15*(1 Pt 1), 70–86. https://doi.org/10.1523/JNEUROSCI.15-01-00070.1995

Taube, J. S., & Burton, H. L. (1995). Head direction cell activity monitored in a novel environment and during a cue conflict situation. *Journal of Neurophysiology*, *74*(5), 1953–1971. https://doi.org/10.1152/JN.1995.74.5.1953

Valenstein, E., Bowers, D., Verfaellie, M., Heilman, K. M., Day, A., & Watson, R. T. (1987). Retrosplenial amnesia. *Brain*, *110*(Pt 6), 1631–1646. https://doi.org/10.1093/brain/110.6.1631

Van Groen, T, Vogt, B. A., & Wyss, J. M. (1993). Interconnections between the thalamus and retrosplenial cortex in the rodent brain. In B. A. Vogt & M. Gabriel (Eds.), *Neurobiology of cingulate cortex and limbic thalamus*. (pp. 478–523). Birkhauser.

Van Groen, T., & Wyss, J. M. (2003). Connections of the retrosplenial granular b cortex in the rat. *Journal of Comparative Neurology*, *463*(3), 249–263. https://doi.org/10.1002/cne.10757

Vann, S. D., Aggleton, J. P., & Maguire, E. A. (2009). What does the retrosplenial cortex do? *Nature Reviews Neuroscience*, *10*(11), 792–802. https://doi.org/10.1038/nrn2733

Vedder, L. C., Miller, A. M. P., Harrison, M. B., & Smith, D. M. (2017). Retrosplenial cortical neurons encode navigational cues, trajectories and reward locations during goal directed navigation. *Cerebral Cortex*, *27*(7), 3713–3723. https://doi.org/10.1093/cercor/bhw192

Wilber, A. A., Clark, B. J., Forster, T. C., Tatsuno, M., & McNaughton, B. L. (2014). Interaction of egocentric and world-centered reference frames in the rat posterior parietal cortex. *The Journal of Neuroscience*, *34*(16), 5431–5446. https://doi.org/10.1523/JNEUROSCI.0511-14.2014

Wilent, W. B., & Nitz, D. A. (2007). Discrete place fields of hippocampal formation interneurons. *Journal of Neurophysiology*, *97*(6), 4152–4161. https://doi.org/10.1152/jn.01200.2006

Wood, E. R., Dudchenko, P. A., Robitsek, R. J., & Eichenbaum, H. (2000). Hippocampal neurons encode information about different types of memory episodes occurring in the same location. *Neuron*, *27*(3), 623–633. https://doi.org/10.1016/S0896-6273(00)00071-4

Wyss, J. M., & Van Groen, T. (1992). Connections between the retrosplenial cortex and the hippocampal formation in the rat: A review. *Hippocampus*, *2*(1), 1–11. https://doi.org/10.1002/hipo.450020102

Zhang, N., Grieves, R. M., & Jeffery, K. J. (2022). Environment symmetry drives a multidirectional code in rat retrosplenial cortex. *The Journal of Neuroscience*, *42*(49), 9227–9241. https://doi.org/10.1523/JNEUROSCI.0619-22.2022

SUPPORTING INFORMATION

Additional supporting information can be found online in the Supporting Information section at the end of this article.

How to cite this article: Subramanian, D. L., Miller, A. M. P., & Smith, D. M. (2024). A comparison of hippocampal and retrosplenial cortical spatial and contextual firing patterns. *Hippocampus*, 1–21. https://doi.org/10.1002/hipo.23610